

**MODE LOCKED ERBIUM DOPED FIBER LASER USING  
ZINC OXIDE THIN FILM AS SATURABLE ABSORBER**

**IBRAHIM ABDULRAHMAN MAHMOOD**

**FACULTY OF ENGINEERING  
UNIVERSITY OF MALAYA  
KUALA LUMPUR**

**2018**

**MODE LOCKED ERBIUM DOPED FIBER LASER  
USING ZINC OXIDE THIN FILM AS SATURABLE  
ABSORBER**

**IBRAHIM ABDULRAHMAN MAHMOOD**

**RESEARCH REPORT SUBMITTED IN PARTIAL  
FULFILMENT OF THE REQUIREMENTS FOR THE  
DEGREE OF MASTER OF TELECOMMUNICATION  
ENGINEERING**

**FACULTY OF ENGINEERING  
UNIVERSITY OF MALAYA  
KUALA LUMPUR**

**2018**

**UNIVERSITY OF MALAYA**  
**ORIGINAL LITERARY WORK DECLARATION**

Name of Candidate: Ibrahim Abdulrahman Mahmood

Matric No: KQH160005

Name of Degree: Master of Telecommunication Engineering

Title of Research Report: Mode Locked Erbium Doped Fiber Laser Using Zinc Oxide Thin Film as Saturable Absorber

Field of Study:

I do solemnly and sincerely declare that:

- (1) I am the sole author/writer of this Work;
- (2) This Work is original;
- (3) Any use of any work in which copyright exists was done by way of fair dealing and for permitted purposes and any excerpt or extract from, or reference to or reproduction of any copyright work has been disclosed expressly and sufficiently and the title of the Work and its authorship have been acknowledged in this Work;
- (4) I do not have any actual knowledge nor do I ought reasonably to know that the making of this work constitutes an infringement of any copyright work;
- (5) I hereby assign all and every rights in the copyright to this Work to the University of Malaya ("UM"), who henceforth shall be owner of the copyright in this Work and that any reproduction or use in any form or by any means whatsoever is prohibited without the written consent of UM having been first had and obtained;
- (6) I am fully aware that if in the course of making this Work I have infringed any copyright whether intentionally or otherwise, I may be subject to legal action or any other action as may be determined by UM.

Candidate's Signature

Date:

Subscribed and solemnly declared before,

Witness's Signature

Date:

Name:

Designation

# MODE LOCKED ERBIUM DOPED FIBER LASER USING ZINC OXIDE THIN FILM AS SATURABLE ABSORBER

## ABSTRACT

Mode locked fiber lasers have attracted a great research interest in recent years due to their applications in many areas such as material processing, remote sensing, optical clock technology and ultrahigh-speed optical communications. Compared with Q-switched fiber lasers, they have the advantages of higher repetition rate, higher peak power, wider spectral range and shorter pulse width. Zinc oxide (ZnO) has also been identified as an ideal saturable absorber (SA) due to its high nonlinear optical response, high sustainability to damage threshold and fast recovery time. In this work, for the first time, two types of mode locked erbium doped fiber lasers (EDFLs) have been experimentally demonstrated using ZnO as SA. At first, the ZnO fabricated into a thin film using a seeding solution mixed with Polyvinyl Alcohol (PVA), was integrated into an EDFL cavity with 201.5 m long optical resonator. Self-started mode locked pulses of 400 ns pulse width was successfully realized at a relatively low pump power of 45.4 mW with the fundamental frequency of 993 kHz. The laser operated at a central wavelength of 1558.34 nm with the pulse energy of 11.6 nJ and peak power of 27.3 mW are obtained at the maximum pump power of 142 mW. The same ZnO SA film was also integrated into another EDFL cavity with a shorter length of 61.5 m. At a pump power of 42 mW, self-started mode locked pulses train was also successfully generated with a much higher repetition rate and much shorter pulse width of 3.26 MHz and 1.76 ps, respectively. The laser operates at a longer wavelength of 1599.5 nm. The pulse energy and peak power of the laser output were 2.16 nJ and 1.14 kW respectively at the maximum pump power of 159 mW while the average output power was obtained at 6.91 mW. This finding indicates

that ZnO thin film is a promising SA material for a demonstration of mode locked EDFL, which may find suitable applications in the emerging optical communication system.

**Keywords:** fiber laser, mode locking, saturable absorber, Zinc Oxide thin film.

University of Malaya

# PERANTI GENTIAN LASER MODE LOCKED MENGGUNAKAN PERYERAP TEPU FILIM NIPIS ZINK OKSIDA

## ABSTRAK

Gentian laser mode-locked telah menarik minat penyelidikan yang hebat dalam beberapa tahun kebelakangan ini kerana peranan mereka yang sangat penting dalam pelbagai aplikasi seperti pemprosesan material, penderiaan jauh, teknologi jam optik dan komunikasi optik kelajuan tinggi. Berbanding dengan laser serat Q-bertukar, mereka mempunyai kelebihan kadar pengulangan yang lebih tinggi, kuasa puncak yang lebih tinggi, jarak spektrum yang lebih luas dan lebar denyut yang lebih pendek. Selain itu, laser serat yang dikunci secara pasif lebih disukai berbanding teknik aktif untuk kelebihan menarik reka bentuk mereka yang mudah, lebih murah, bebas daripada penjajaran, dan kestabilan yang baik. Baru-baru ini, ZnO telah dikenalpasti sebagai penyerap yang saturable ideal (SA) disebabkan oleh tindak balas optik bukan linear yang tinggi, kelestarian yang tinggi untuk merosakkan ambang dan masa pemulihan yang cepat. Dalam kerja ini, untuk pertama kalinya, dua jenis mod dikunci erbium laser serat doped (EDFLs) telah ditunjukkan secara eksperimen menggunakan zink oksida (ZnO) nanopartikel sebagai SA. Pada mulanya, ZnO dibuat ke dalam filem nipis menggunakan penyelesaian pembenihan dan digabungkan dalam resonator optik panjang 201.5 m sistem laser. Mod mulailah dikunci denyut nadi pulsa 400 ns direalisasikan pada kuasa pam yang agak rendah sebanyak 45.4 mW, dan frekuensi asas adalah 993 kHz. Walaupun panjang gelombang pusat diukur pada 1558.34 nm. Selain itu, tenaga denyut laser dan kuasa puncak yang dicadangkan pada kuasa pam yang maksimum sebanyak 142 mW dianggarkan masing-masing 11.6 nJ dan 27.3 mW. Oleh itu, keputusan ini menunjukkan bahawa nanopartikel ZnO adalah SA yang menjanjikan untuk menghasilkan mod nanosecond yang dikunci EDFL untuk aplikasi yang memerlukan tenaga nadi yang tinggi

dan kuasa output purata. Kemudian, dalam eksperimen lain, nanopartikel ZnO fabrikasi yang sama dibuat di dalam rongga laser yang berbeza dengan panjang lebih pendek 61.5 m. Mod permulaan dikunci denyutan telah dijana dengan kadar pengulangan yang jauh lebih tinggi dan lebar nadi yang lebih pendek daripada 3.26 MHz dan 1.76 ps, masing-masing, dengan kuasa pam 42 mW. Laser beroperasi dalam band panjang gelombang panjang (L-band) dengan panjang gelombang pusat 1599.5 nm. Tenaga nadi dan kuasa puncak output laser telah dianggarkan pada 2.16 nJ dan 1.14 kW masing-masing pada kuasa pam maksimum 159 mW di mana kuasa output purata ialah 6.91 mW. Berdasarkan hasil ini, kami percaya bahawa laser yang dicadangkan dapat dilihat sebagai sumber cahaya yang menjanjikan dalam sistem komunikasi optik yang muncul.

**Kata kunci:** laser serat, penguncian mod, penyerap basah, Zink oksida filem tipis.

## ACKNOWLEDGEMENTS

First and foremost, all praise is due to Allah, the most compassionate and the most merciful, who enables me and give me the strength and health to do this work, then all the praise to the holy prophet Muhammad (peace be upon him), the city of knowledge. Secondly, I would like to express my huge grateful and thankful to my parents, my brothers and my sisters, whose love, support and guidance are with me in whatever I pursue. Thirdly, I offer my sincerest gratitude to my supervisor, Prof. Ir. Dr. Sulaiman Wadi Harun, who has supported me throughout my research project with his patience and knowledge whilst allowing me the room to work in my own way. One simply could not wish for a better or friendlier supervisor.

My sincere thanks also go to Dr. Mahmoud Hazzaa Mohammed Ahmed, Dr. Ahmed Hasan Hamood Al-Masoodi, Mr. Muhammad Quisar Lokman and Dr. Anas Abdul Latiff, who provided me an opportunity to join their team as intern, and for their patience and support in overcoming numerous obstacles I have been facing through my research. Without their precious support, it would not be possible to conduct this research.

Special mention goes to Ms. Reham Abdulkareem for the infinity support, motivate and care along the way of my master degree, which is only the tip of the iceberg. Finally, many thanks should go to whoever contributed, directly or indirectly, in producing the final form of the present work, especially my friends.

Thank you!



## TABLE OF CONTENTS

Abstract .....	ii
Abstrak .....	iv
Acknowledgements .....	vi
Table of Contents .....	vii
List of Figures .....	ix
List of Symbols and Abbreviations .....	xi
<b>CHAPTER 1: INTRODUCTION .....</b>	<b>1</b>
1.1 Background of fiber laser .....	1
1.2 Problem statement .....	2
1.3 Objectives .....	4
1.4 Research Contribution .....	4
1.5 Report's outline .....	5
<b>CHAPTER 2: LITERATURE REVIEW .....</b>	<b>6</b>
2.1 Overview of laser .....	6
2.1.1 Working principle of laser .....	6
2.1.2 Laser Components .....	7
2.2 Fiber lasers .....	9
2.3 Erbium doped fiber .....	10
2.4 Pulsed lasers .....	12
2.4.1 Q-switching .....	13
2.4.2 Mode locking .....	14
2.5 Saturable absorbers .....	19
2.5.1 Zinc Oxide (ZnO) .....	23

**CHAPTER 3: NANOSECOND MODE-LOCKED ERBIUM DOPED FIBER  
LASER BASED ON ZINC OXIDE THIN FILM AS A SATURABLE ABSORBER**

**26**

3.1	Introduction.....	26
3.2	The Fabrication of Zinc Oxide Thin Film .....	27
3.3	Characterization of ZnO thin film .....	28
3.3.1	Field emission scanning electron microscopy (FESEM) .....	29
3.3.2	Raman spectrum .....	29
3.3.3	Linear optical absorption.....	30
3.3.4	Nonlinear optical absorption .....	32
3.4	Experimental setup .....	33
3.5	Results and Discussion .....	35
3.6	Summary.....	38

**CHAPTER 4: PICOSECONDS MODE-LOCKED ERBIUM DOPED FIBER  
LASER BASED ON ZINC OXIDE THIN FILM AS SATURABLE ABSORBER 39**

4.1	Introduction.....	39
4.2	Experimental setup .....	40
4.3	Mode-locking performance .....	41
4.4	Summary.....	45

**CHAPTER 5: CONCLUSION..... 46**

References .....	48
List of Publications and Papers Presented .....	55

## LIST OF FIGURES

Figure 2.1 (a) absorption (b) spontaneous emission (c) stimulated emission .....	7
Figure 2.2 laser components .....	8
Figure 2.3 Main components of fiber laser .....	10
Figure 2.4 Erbium transition diagram .....	12
Figure 2.5 operation of passive Q-switching .....	14
Figure 2.6 (a) Five individual modes with random phases (b) output of the laser .....	16
Figure 2.7 (a) Five indivisible modes with the same phase (b) output of the laser .....	17
Figure 2.8 The main components for active mode locked laser .....	18
Figure 2.9 The main comments of passively mode locking .....	19
Figure 2.10 The historical evolution of the saturable absorber technologies (the balls in blue color indicate the nanomaterials) .....	22
Figure 2.11 The hexagonal wurtzite structure of ZnO. O atoms are shown as large white spheres, Zn atoms as smaller black spheres. One unit cell is outlined for clarity.....	24
Figure 3.1 Fabrication process of ZnO thin film saturable absorber .....	28
Figure 3.2 FESEM images. Insert shows a high magnification of the image .....	29
Figure 3.3 Raman spectrum of ZnO-PVA .....	30
Figure 3.4 The configuration of the linear absorption experiments.....	31
Figure 3.5 Linear absorption spectrum of the ZnO based SA.....	31
Figure 3.6 The setup of the dual-detector technique.....	32
Figure 3.7 Nonlinear absorption of the ZnO SA.....	33
Figure 3.8 Experimental setup of the proposed mode locked EDFL.....	34
Figure 3.9 Output spectrum of mode-locked EDFL at pump power of 142 mW .....	35
Figure 3.10 (a)The oscilloscope trace of the mode-locked EDFL at pump power of 142 mW (b) single envelope of the pulse .....	36

Figure 3.11 RF spectrum of the mode locked at 142 mW .....	37
Figure 3.12 Output power and pulse energy as a function of 980nm pump power. ....	37
Figure 4.1 Experimental setup of the proposed mode locked EDFL for picosecond pulse generation.....	41
Figure 4.2 Output spectrum of mode-locked EDFL at a pump power of 159 mW. ....	42
Figure 4.3 The oscilloscope trace of the mode-locked EDFL at a pump power of 159 mW. ....	42
Figure 4.4 Autocorrelation trace of the mode-locked EDFL at a pump power of 159 mW. ....	43
Figure 4.5 RF spectrum of the mode locked at 159 mW. ....	44
Figure 4.6 Output power and pulse energy as a function of 980nm pump power .....	44

University of Malaya

## LIST OF SYMBOLS AND ABBREVIATIONS

BP	:	Black Phosphorus
$c$	:	Speed of light
C-band	:	Conventional band
CO <sub>2</sub>	:	Carbone Dioxide
CNTs	:	Carbone Nanotubes
EDF	:	Erbium Doped Fiber
EDFL	:	Erbium Doped Fiber Laser
Er	:	Erbium
FESEM	:	Field Emission Scanning Electron Microscopy
FWHM	:	Full Width Half Maximum
GVD	:	Group Velocity Dispersion
He-Ne	:	Helium–Neon
LD	:	Laser Diode
L	:	Cavity length
L-band	:	Long band
LO	:	Longitudinal Optical
MQW	:	Multiple Quantum Well
MASER	:	Microwave Amplification by Stimulated Emission of Radiation
MOS <sub>2</sub>	:	Molybdenum disulfide
N	:	Number of modes
NOLM	:	Nonlinear-Optical Loop Mirror
NA	:	Numerical Aperture
NPR	:	Nonlinear Polarization Rotation
O	:	Oxygen

OSA	:	Optical Spectrum Analyzer
OSC	:	Oscilloscope
OC	:	Optical Coupler
PVA	:	Polyvinyl Alcohol
QD	:	Quantum Dot
RF	:	Radio Frequency
SNR	:	Signal to Noise Ratio
SMF	:	Single Mode Fiber
SESAM	:	Semiconductor Saturable Absorber Mirrors
SWCNTs	:	Single Wall Carbon Nanotubes
TI	:	Topological Insulator
TO	:	Transverse Optical
TMD	:	Transition Metal Dichalcogenides
VOA	:	Variable Optical Attenuator
WDM	:	Wavelength Division Multiplexer
WS <sub>2</sub>	:	Tungsten disulfide
Yb	:	Ytterbium
Yb-Er	:	Ytterbium-Erbium
Zn	:	Zinc
ZnO	:	Zinc Oxide
$\tau$	:	Pulse duration
$\Delta t$	:	Pulse width
$\Delta \nu$	:	Operation frequency
0D	:	Zero Dimensional
1D	:	One Dimensional

2D : Two Dimensional

3D : Three Dimensional

University of Malaya

## CHAPTER 1: INTRODUCTION

### 1.1 Background of fiber laser

Since been built for the first time in 1960, lasers have found its importance in many applications Such as optical communication system, sensors, medicine, industry, and military (Fermann et al., 2002). Broadly, we can characterize Lasers according to their active medium into gas lasers such as a CO<sub>2</sub> laser, liquid lasers such as dye laser, and solid-state lasers such as semiconductor lasers and fiber lasers. However, fiber lasers are preferred on the other types of lasers because of the advantages of reliability, compactness, zero alignments, low cost and can provide high output and peak power (Dong & Samson, 2016). Moreover, since the gain medium is an optical fiber, it can be smoothly coupled into the optical communication system with the lowest possible coupling loss. Due to these merits, fiber lasers become essential in many fields such as engineering technology, laser welding, cutting, and folding of metals, 3D printing, spectroscopy, medicine and optical communication.

Fiber lasers can operate in various ranges of wavelengths depending on the type of the rare earth material that used in doping the fiber. The most commonly rare earth materials that used in forming the active mediums of the fiber lasers are ytterbium, erbium, thulium operating in 1 $\mu$ m, 1.5 $\mu$ m, 2 $\mu$ m wavelength regions, respectively. However, erbium doped fiber lasers (EDFLs) are the most developed fiber lasers where they gain huge interest for fiber sensor and optical communication applications. Normally, fiber lasers can operate in either continuous wave (CW) or pulsed modes. pulsed lasers have got more attention by researchers than CW lasers due to the large range of applications that can be used for such as laser surgery, industrial, range finding, optical communication and fiber sensing. Pulsed fiber lasers are constructing using either Q-switching or mode locking mechanisms. Q-switching simply can be defined as a technique of producing extremely short pulses of light with high peak power which is higher than that could be produced



by similar laser operates in CW mode through the modulating of the loss inside the laser cavity. While mode locking technique produces ultrafast pulses of light with much higher peak power than Q-switching technique through the locking of the oscillating modes inside the laser cavity. Those ultrafast fiber lasers have an important role in many fields such as medicine, industry, remote sensing and optical communication (Altshuler et al., 2004; Ding et al., 2017; Mizrahi et al., 1993).

## **1.2 Problem statement**

Mode-locking is a technique in optics by which a fiber laser can be made to produce pulses of light of extremely short duration, as short as few picoseconds or femtoseconds. One technique of realizing mode locked laser is by inserting inside the laser's optical resonator an active element such as acousto-optic or electro optic modulator which acts as an optical modulator to periodically modulate the losses or the round-trip phase (J-H Lin et al., 2010; Swann et al., 2011). However, the presence of the modulator and bulk devices in the cavity makes this technique complicated. Another simple, low cost and accessible technique is by using saturable absorber (SA) which is recently become the most interesting research in producing passive mode-locked fiber laser.

To date, many types of SAs have been investigated and used to implement mode locking fiber laser such as Semiconductor Saturable Absorption Mirrors (SESAMs) (Qingsong et al., 2017; X. Sun et al., 2017), Nonlinear Polarization Rotation (NPR) (C. Gao et al., 2017; A. P. Luo et al., 2011), Nonlinear-Optical Loop Mirror (NOLM) (Cai et al., 2017; Zhong et al., 2010). Yet, each of these SAs has some limitations: SESAM is complex to fabricate, costly, narrow operation wavelength range and the response time is limited. NPR has a limited particular application because of its sensitivity to the ambient such as variation of temperature or vibration. NOLM needs long fiber to provide sufficient nonlinear phase shift. Therefore, that have been pushed up the researchers

forward to intensively investigate new candidates to realize passive mode locked fiber laser.

In the last decade, CNT and graphene have become the most attracted materials to the researchers because of their advantages of low cost, simple to fabricate, ultra-fast recovery time and operate in the wide wavelength band (M. Ahmed et al., 2014; Z. Sun et al., 2010). However, it is complex to control the bandgap of the CNT which limit their operating range. On the other hand, graphene has zero bandgap, low damage threshold and its absorption co-efficiency is relatively low. Due to these limitations, other materials have been proposed and intensively investigated such as topological insulators (TIs), transition-metal dichalcogenides (TMDs) and transition metal oxides which are classified as a nanomaterial. Last few years, many TIs have been reported and constructed as SAs such as bismuth selenide ( $\text{Bi}_2\text{Se}_3$ ) (L. Gao et al., 2015), antimony telluride ( $\text{Sb}_2\text{Te}_3$ ) (Boguslawski et al., 2015) and bismuth telluride ( $\text{Bi}_2\text{Te}_3$ ) (Yin et al., 2015), and TMDs, such as tungsten disulphide ( $\text{WS}_2$ ) (Mao et al., 2015), tungsten diselenide ( $\text{WSe}_2$ ) (Mao et al., 2016), molybdenum disulphide ( $\text{MoS}_2$ ) (M. Ahmed et al., 2016), and molybdenum diselenide ( $\text{MoSe}_2$ ) (Z. Luo et al., 2015). Nevertheless, some optical constraints are still excited such as a relatively wide bandgap of TMD nanomaterials which is more preferred within the visible light range and complex fabrication process of TI nanomaterials (Song et al., 2017).

Recently, black phosphorous as a novel 2D material has also reported as a promising SA for both Q-switched and mode locked fiber lasers applications (Song et al., 2017). Black phosphorus defers from the other types of 2D materials by having a controllable bandgap through the control of its thickness which is a useful property for the electrooptic applications. However, in case of long time exposure, black phosphorous might be a hazard to human health. Furthermore, when high power illuminates the black

phosphorous, its oxidation will be accelerated in the air which leads to optical damage and thermal effect; and will consequently decrease its damage threshold (Feng et al., 2016). Hence, to this point, the investigation for new SA candidates with better performance is still a very attractive topic for the researchers.

### **1.3 Objectives**

The aim of this report is to develop a new mode locked EDFL using zinc oxide thin film as a novel transition metal oxide saturable absorber. To achieve this aim, this research is being guided by the following objectives:

1. To fabricate and characterize Zinc Oxide thin film based saturable absorber.
2. To demonstrate mode locked EDFL using the fabricated ZnO saturable absorber.

### **1.4 Research Contribution**

Ultra violet laser diodes, thin-film transistors, nanotechnology based devices, light-emitting diodes and transparent electrodes in liquid crystal displays are the electro-optical applications that have used ZnO due to its important properties such as bio-safe, radiation hardness, low power threshold for optical pumping and wet chemical etching (Janotti & Van de Walle, 2009). However, only recently, ZnO with a direct band-gap of 3.4eV (Jagadish & Pearton, 2011) and exciton binding energy of 60 meV at room temperature (Bagnall et al., 1997) has been seen as an ideal SA candidate due to its high sustainability to damage threshold, high nonlinear optical response, simple fabrication process, fast recovery time and environment friendly (Ahmad, Lee, Ismail, Ali, Reduan, Ruslan, Ismail, et al., 2016; Jamdagni et al., 2016).

To date, Q-switched fiber lasers have been constructed and reported using ZnO as a SA (Ahmad, Lee, Ismail, Ali, Reduan, Ruslan, & Harun, 2016; Ahmad, Lee, Ismail, Ali, Reduan, Ruslan, Ismail, et al., 2016; Ahmad, Salim, et al., 2016; Aziz et al., 2017).

However, to the best of my knowledge, no mode locked EDFL using ZnO as SA has been reported yet. In this report, two mode locked EDFLs based ZnO thin film as saturable absorber have been experimentally constructed for the first time. The first reported laser operates in the conventional band wavelength (C-band) of 1558.34 nm and a pulse width of nanoseconds duration. While the second reported laser operates in the long band wavelength (L-band) of 1599.5 nm and a pulse width of picoseconds duration.

## **1.5 Report's outline**

Generally, this report presents the overview, working principle, mechanism, experimental results and discussion of the developed mode locked EDFLs based on ZnO thin film as a saturable absorber. It consists of 5 chapters. The background, problem statement, research contribution, and objectives are presented in the first chapter. The second chapter provides a very simple overview of the laser operation and its components, the advantages of fiber lasers over the other types of laser, the working principle of erbium doped fiber, brief discussion about the two mechanisms of constructing pulsed lasers, the function of the saturable absorbers in producing passively mode locked fiber laser and the importance of zinc oxide SA over the other types of SAs. In the third chapter, the fabrication process and the characterization of the ZnO thin film are introduced first, then the fabricated ZnO-SA is used to construct nanosecond mode locked EDFL and the results of this experiment are presented and discussed as well. While the fourth chapter describes and discusses the demonstration of the picosecond mode locked EDFL based ZnO thin film saturable absorber. Finally, the last chapter ends this report by concluding the work.

## **CHAPTER 2: LITERATURE REVIEW**

### **2.1 Overview of laser**

A laser is a simple however very powerful device that emits a coherent light with extremely narrow beam width by utilizing the process of optical amplification based on the stimulated emission of electromagnetic radiation. Laser stands for "light amplification by stimulated emission of radiation". Since been built for the first time in 1960, lasers have found its importance in many applications Such as optical communication, sensors, medicine, industry, and military (Fermann et al., 2002). Even though laser light and ordinary light are both electromagnetic waves, they largely differ from each other. Ordinary light travels in all directions, consist of all wavelengths and incoherent whereas light produced by the laser is highly directional, monochromatic and coherent. Therefore, laser light can travel much further distance and can be concentrated on very small area than ordinary lights. Those unique properties of lasers have made them essential devices for cutting and welding materials, optical disk drives, barcode scanners, laser surgery and skin treatments, range finding and communication (Cantello et al., 2001).

#### **2.1.1 Working principle of laser**

In fact, the idea of the laser was inspired by the working principle of the microwave amplification by stimulated emission of radiation (MASER) which was first invented in 1953 by Charles Townes at Columbia University. When in 1958, this idea was extended from microwave to the optical frequencies by Townes and Schawlow. where they have developed an optical amplifier through the growth of the beam inside a resonator cavity formed by optical mirrors. Then two years later, the first laser is built by Theodore H. Maiman at Hughes Research Laboratories based on previous theoretical work of Townes and Schawlow (Maiman, 1960; Silfvast, 2004). Basically, the operation mechanism of the laser depends on three main processes which are absorption, spontaneous emission and stimulated emission as shown in Figure 2.1. Initially, atoms love to stay at the lowest

energy level. However, when those atoms illuminated by an external energy source they will be excited from the lower energy level ( $E_1$ ) into higher energy level ( $E_2$ ) through absorbing that energy. Therefore, this process called absorption as drawn in Figure 2.1 (a). Then, since those atoms got extremely short live time in the excited state they will decay back to the lower energy level  $E_1$  and emit photons through spontaneous or stimulated emission. If there is an incoming photon which has an energy exactly equal to the energy difference between  $E_1$  and  $E_2$ , the stimulated emission will take place, else if the spontaneous emission will occur. The photons emitted through the spontaneous emission are random, out of phase and travel in all directions as indicated in Figure 2.1 (b). Those emitted through the stimulated emission are coherent, in phase and travel in one direction as shown in figure 2.1 (c). Therefore, photons generated through stimulated emission are responsible for the amplification and consequently lasing (Svelto & Hanna, 1998).

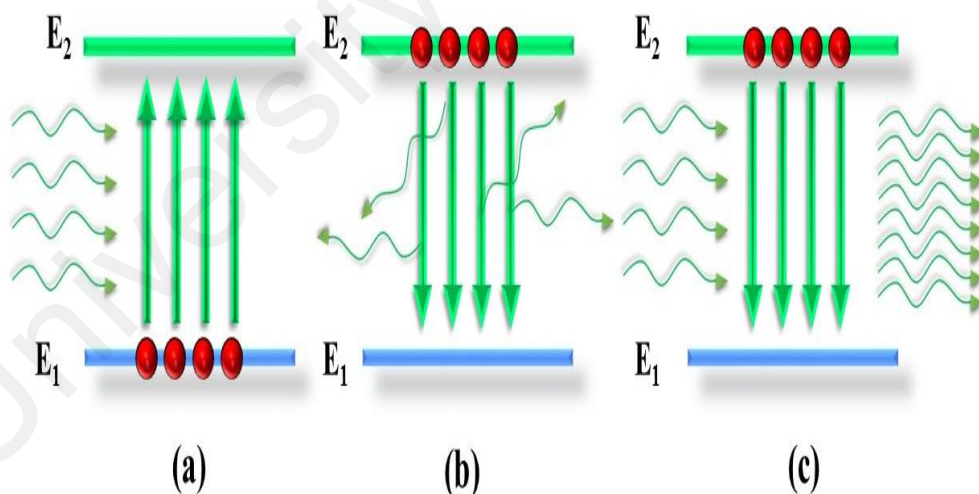


**Figure 2.1 (a) absorption (b) spontaneous emission (c) stimulated emission**

### 2.1.2 Laser Components

In order to achieve the stimulated emission which is necessary for lasing, an active medium is required to support the population inversion process. The active medium or the gain medium considers the major factor for determining the operation wavelength of

the laser. It could be either gas, liquid or solid. Secondly, we must have a pumping mechanism to provide the adequate energy to the active medium to achieve the population inversion. The pump source could be electrical, optical, chemical or thermal in nature which mainly depends on the type of the active medium used. For example, gas lasers usually use electrical discharge as a pump source while solid state lasers are optically pumped using flashlamps or semiconductor laser diodes. After achieving the population inversion and photons been generated through the stimulated emission, it is very important to amplify the produced photons by feeding them back into the active medium. This optical feedback could be made by integrated two mirrors at the ends of the active medium formed the optical resonator. In addition to the design and alignment of the mirrors with respect to the medium is crucial. One of the mirrors has 100% reflection, while the other mirror is partially reflector to allow some of the light to pass through as an output (Quimby, 2006). The basic structure of the laser system is shown in Figure 2.2.

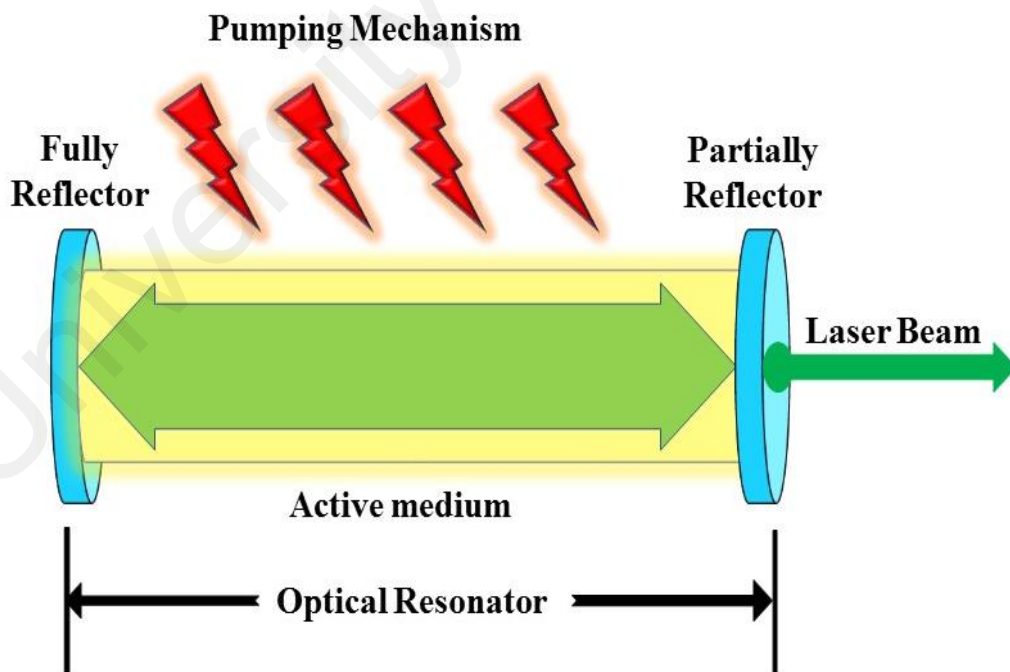


Figure 2.2 laser components

## 2.2 Fiber lasers

Lasers can be characterized according to their active medium into gas lasers, liquid lasers, and solid lasers such as semiconductor lasers and fiber lasers. However, fiber lasers are preferred on the other types of lasers because of the advantages of reliability, compactness, low cost and can provide high output and peak power (Dong & Samson, 2016). Furthermore, since the light in fiber lasers is already traveled inside the fiber, it needs zero alignments. Therefore, it can be easily integrated into a movable focusing element that is important for applications such as laser welding, cutting, and folding of metals (Ter-Mikirtychev, 2013). Moreover, it can be smoothly coupled into the optical communication system. Fiber lasers are the lasers which utilize the optical fiber doped with rare-earth elements such as erbium, ytterbium, neodymium, dysprosium, praseodymium, thulium, and holmium as gain mediums (Dong & Samson, 2016). Each of these rare earth elements provides gain in a specified wavelength range for example erbium works in 1550 nm which is the most remarkable for optical communication while ytterbium operates in 1000 nm which is mainly used for industry (Chong et al., 2006; Mizrahi et al., 1993).

Usually, fiber laser can be configured using either linear or ring cavity however in this report we only focusing on ring cavity as drawn in Figure 2.3. The most commonly pump sources of the fiber lasers are semiconductor laser diodes (LDs) because they are very compact, efficient and cheap in addition to the availability of all the desirable wavelengths that are essential for the amplification process inside the active medium. Wavelength division multiplexer (WDM) is used to couple the pump beam into the active medium together with the feedback. Finally, an optical coupler (OC) is used to feed part of the light back to the cavity for the purpose of the amplification and extract the rest as output. Furthermore, isolator could be used to insure the unidirectionality inside the cavity and prevent the LD from damage (M. Ahmed et al., 2016).



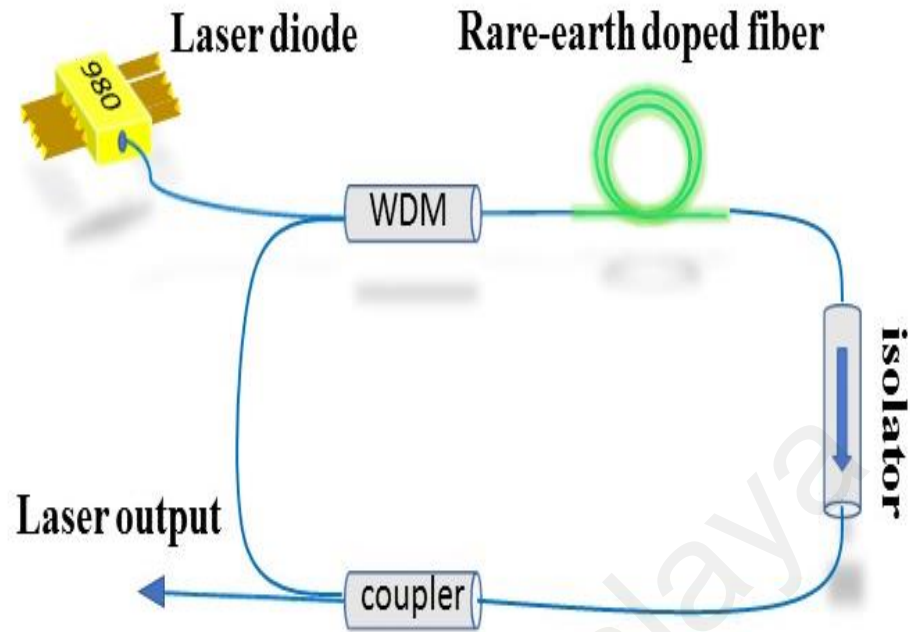


**Figure 2.3 Main components of fiber laser**

### **2.3 Erbium doped fiber**

As mentioned earlier, the erbium ions are the most desirable rare earth element for the optical communication applications to what they provide from the gain in the third communication window where the loss in the optical fiber is very less (R. Mears et al., 1986). Since been fabricated for the first time in 1978 (R. J. Mears et al., 1987), EDFs have been intensively studied and used for construction of both erbium doped fiber amplifier (EDFA) and erbium doped fiber laser (EDFL) that mainly used in the optical communication system (Desurvire et al., 1991; Mizrahi et al., 1993). The energy level diagram of the erbium ions is illustrated in Figure 2.4. As indicated in the figure, the many excited levels mean that erbium ions can be pumped with many different wavelengths which equal to the energy different between the excited level and the ground state

(Laming et al., 1989). However, 1.48  $\mu\text{m}$  and 0.98  $\mu\text{m}$  are the most appropriate wavelengths because they are the fewer energies that could be used to excite erbium ions.

When erbium ions pumped with 1.485  $\mu\text{m}$ , they will be excited from the ground state  $^4I_{15/2}$  directly to the metastable level  $^4I_{13/2}$ . Then within the group of levels of  $^4I_{13/2}$  rapid relaxation would occur to the lowest sub-level where laser action would take place. Therefore, in this case, it is called two levels system owing to only two energy levels are involved in the overall process. While if erbium ions pumped with 0.98  $\mu\text{m}$ , they will be excited from the ground state  $^4I_{15/2}$  to higher unstable excited state  $^4I_{11/2}$  where they will stay for a very short time of approximately 1  $\mu\text{s}$  before they decay to the lower metastable level  $^4I_{13/2}$  through releasing heat. So, it is a non-radiative transition. As a result, population inversion will be achieved between the metastable level and the ground state.

Finally, after spending their lifetime they will make the transition to the ground state through either spontaneous emission or stimulated emission as discussed earlier. So that, at 0.98  $\mu\text{m}$  it is called three levels system owing to three energy levels are involved in the overall process. Despite the optical power conversion efficiency of the 1.485  $\mu\text{m}$  pumping is higher than that of 0.98  $\mu\text{m}$  pumping, yet the latest is highly preferred and used more commonly to what it has from advantages such as low noise, larger population inversion and wider separation between the laser wavelength and pump wavelength (El\_Mashade & Mohamed, 2017).

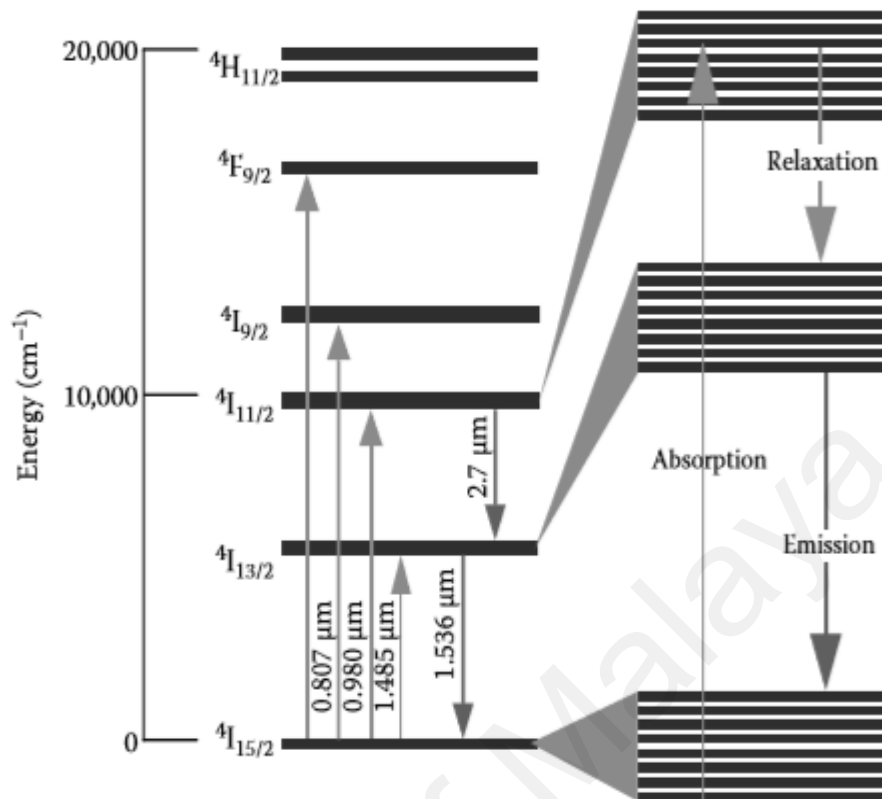


Figure 2.4 Erbium transition diagram (Ngo, 2010)

## 2.4 Pulsed lasers

Clearly, pulsed lasers have got more attention by researchers than continuous wave (CW) lasers due to the large range of applications that can be used in such as laser surgery, industrial, range finding, optical communication and fiber sensing. Pulsed fiber lasers are differing from CW laser in which they release the energy in form of short pulses and high peak power, while the CW lasers release a constant intensity of light over the time (Adel, 2004). Therefore, in pulsed lasers, we usually deal with the parameters such as repetition rate, pulse width, peak power and pulse energy (M. H. M. Ahmed, 2015). Most of the current communication systems and internet networks send and receive data digitally. Consequently, EDFLs which are mainly used for optical communication have to operate in a pulsed mode in order to easily modulate the binary number into optical pulses and vice versa. Logically, faster EDFL means more data can be sent within a short time

leading to speeder internet. Based on this fact, researchers have done a lot of effort on the construction of pulsed EDFLs with extremely short pulse width and high repetition rate. Generally, there are two mechanisms of construction pulsed laser which are Q-switching and mode locking as they discussed below.

#### **2.4.1 Q-switching**

When the width of the pulses needs to be in the order of microsecond or nanosecond, Q-switching technique is usually employed. The Q-switching technique was first described in 1961 by Hellworth where he proposed that laser could produce short pulses if the cavity loss is switching suddenly. Then the year after, McClung and he have experimentally demonstrated Q-switched laser (McClung & Hellwarth, 1962). Therefore, Q-switching simply can be defined as a technique of producing extremely short pulses of light with high peak power which is higher than that could be produced by similar laser operates in CW mode. In theory, a variable attenuator which is commonly known as “Q switcher” is inserting inside the laser’s cavity to generate Q-switching. When this attenuator operates, lasing will not accrue because the light inside the cavity will not be able to oscillate. And that due to the decreasing in the quality factor or Q factor of the cavity. Where low Q factor corresponds to high cavity loss per round trip and vis versa (M. H. M. Ahmed, 2015). This process is illustrated in Figure 2.5. The Q-switching can be achieved either actively or passively based on the variable attenuator used. If the Q switcher is an active element such as an acoustic optic modulator or electro optic modulator, the Q-switching produced is active. While if the Q-switcher used is a passive element such as saturable absorber (SA), the Q-switching, in this case, is passive. The passive Q-switching techniques are preferred over the active one because they got the advantages of simplicity, more stable and low cost (M. H. M. Ahmed, 2015).

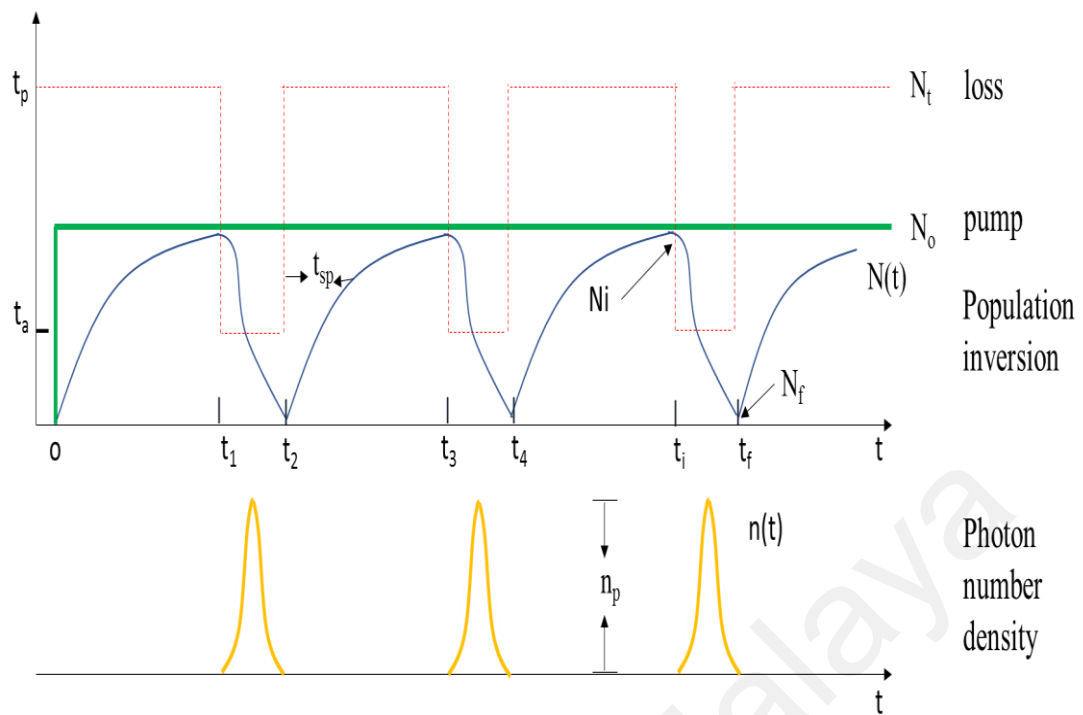


**Figure 2.5 operation of passive Q-switching**

#### 2.4.2 Mode locking

While if the duration of the pulse width needs to be in the order of few picoseconds or femtosecond, mode locking is the best technique to be employed. The idea of the mode locking technique is first being introduced in 1964 by DiDomenico. Where he predicted that mode coupling with well-defined amplitude and phase could result from small signal modulating of cavity loss in a laser at a frequency equal to multiples of axial mode spacing (DiDomenico Jr, 1964). The mode locking of the laser was later titled on this phenomenon. One month later, Hargrove et al. were demonstrated the first mode locked laser by integrated an acoustic optic modulator inside the He-Ne laser's optical resonator. By the time goes on, researchers were investigating more and more about new methods of construction mode locked lasers using different types of laser and various optical modulators. Till the year 1989, Yb–Er-doped fiber laser was presented to release mode locked pulses using AM modulator for the first time (Paschotta et al., 1997). Since that time, mode locked fiber lasers have largely captured the interest of the researchers where

tens of methods have been proposed and reported to demonstrate mode locked fiber lasers in different wavelength ranges for various applications.

Naturally, each laser generates a light consist of a range of frequencies within the operation bandwidth of the gain medium that used in demonstrating that laser. When these frequencies oscillating inside the optical resonator of the laser, they will interfere constructively and destructively with each other producing what are known as standing waves or modes. In fact, these formed modes are the only frequencies that are allowed to oscillate by the cavity while the rest eliminated by the destructive interference. In the normal case, these modes oscillate inside the cavity out of phase which means that there is no fixed relationship between each other as shown in Figure 2.6. In this situation, the interference between these modes will lead to either random output intensity if there are only a few oscillating modes which is known as beating effect, or relatively constant output intensity if there are thousands of oscillating modes in the cavity. The laser, in this case, called continuous wave (CW) laser. While if those modes in such a way oscillated with a fixed relationship with each other or same phase as indicated in Figure 2.7, they will constructively interfere or “locked” with each other producing extremely short pulses of light. The laser, in this case, is called mode locked laser (M. H. M. Ahmed, 2015). The produced pulses are separated with a fixed time that can be calculated using the following equation:

$$\tau = \frac{2L}{c} \quad (2.1)$$

where L is the cavity length while c is the speed of the light inside the cavity. Therefore, the operation frequency ( $\Delta\nu$ ) of the laser can be calculated using the following equation:

$$\Delta\nu = \frac{1}{\tau} \quad (2.2)$$

The pulse width is mainly determined by the number of the looked modes (N). The larger number of looked modes, the shorter pulse width will be. Practically, the pulse width is actually determined based on the shape of the pulse (Ngo, 2010). For instance, if the shape of the pulses is Gaussian temporal shape, the minimum value of the pulse width will be calculated by:

$$\Delta t = \frac{0.441}{N \cdot \Delta \nu} \quad (2.3)$$

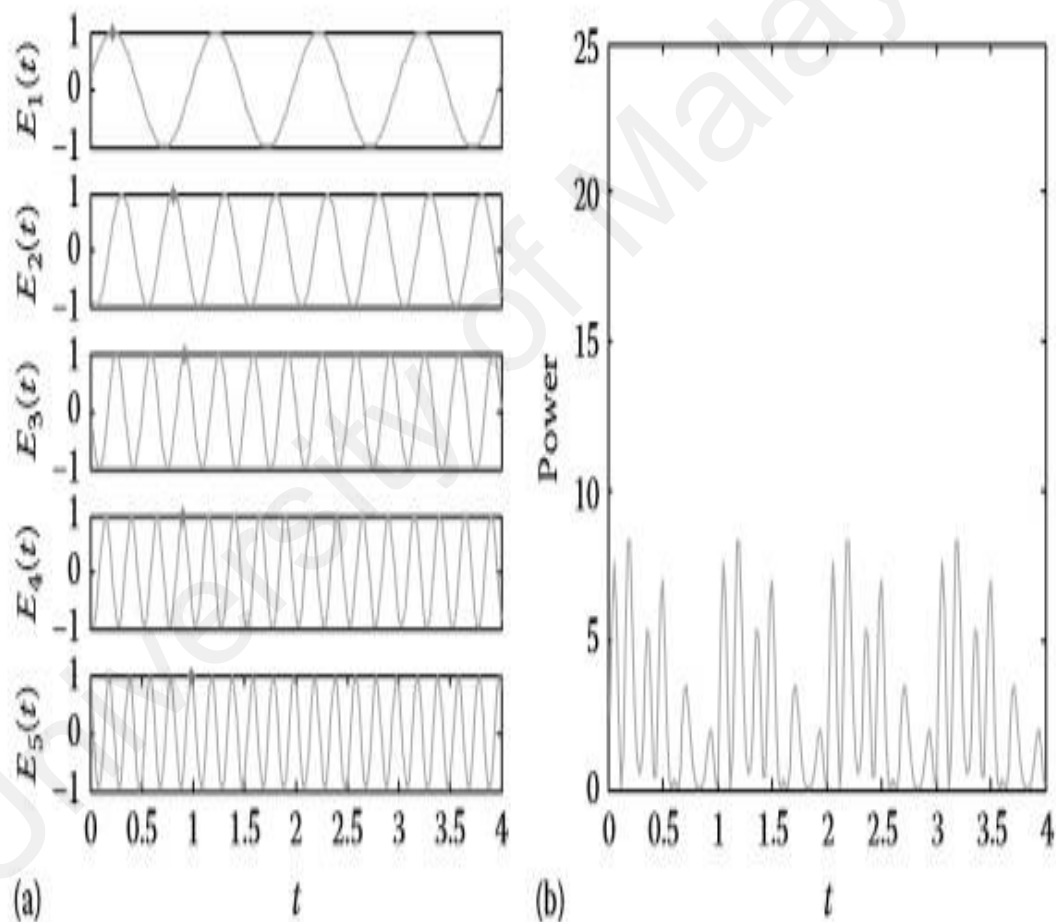


**Figure 2.6 (a) Five individual modes with random phases (b) output of the laser (Ngo, 2010)**

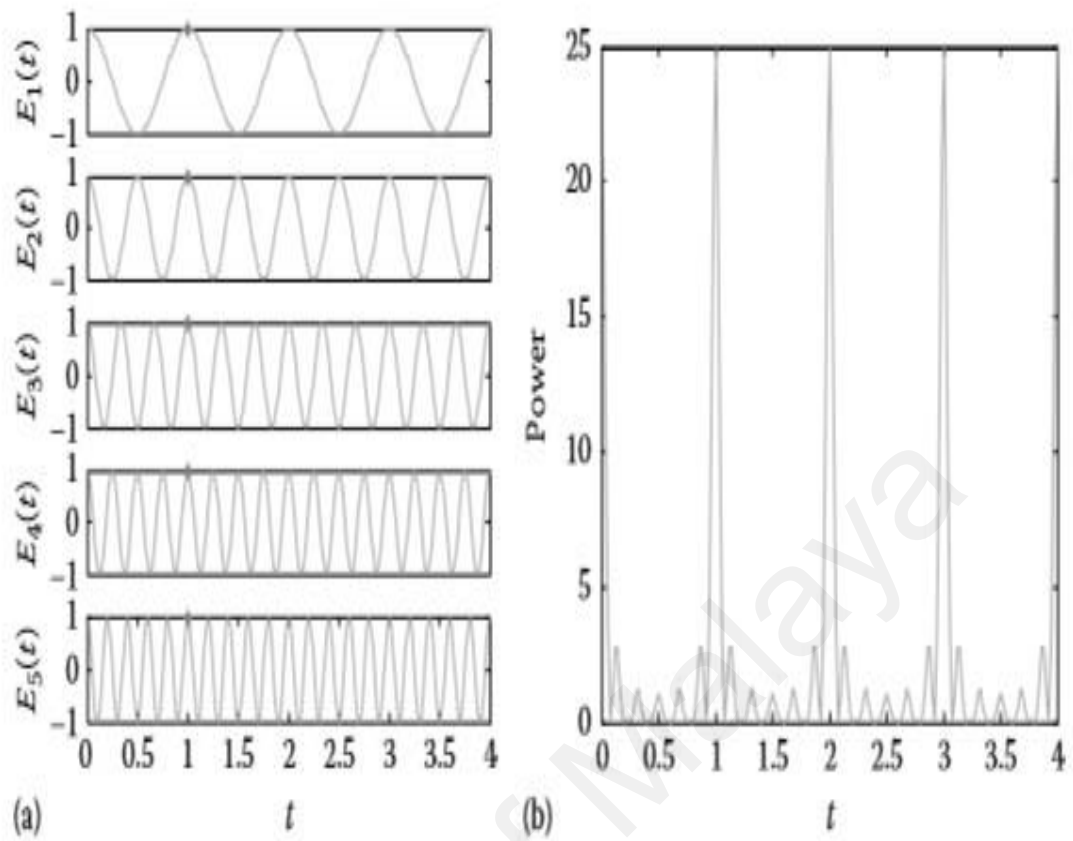


**Figure 2.7 (a) Five indivisible modes with the same phase (b) output of the laser (Ngo, 2010)**

Just like Q-switching, there are many methods for constructing mode locked lasers, we can categorize them into two categories active and passive methods. Active methods generally use an external signal to modulate the light inside the cavity. This is basically achieved by inserting an active element such as electro-optic or acoustic-optic modulators inside the cavity. When these devices are driven with an electrical signal, mode locked pulses will be released through either amplitude modulation or frequency modulation, respectively (Paschotta et al., 1997). The schematic of the actively mode locked laser is drawn in Figure 2.8. However, these methods are relatively expensive, complex and bulky due to the presence of the bulk devices and modulators inside the optical resonator of the laser.



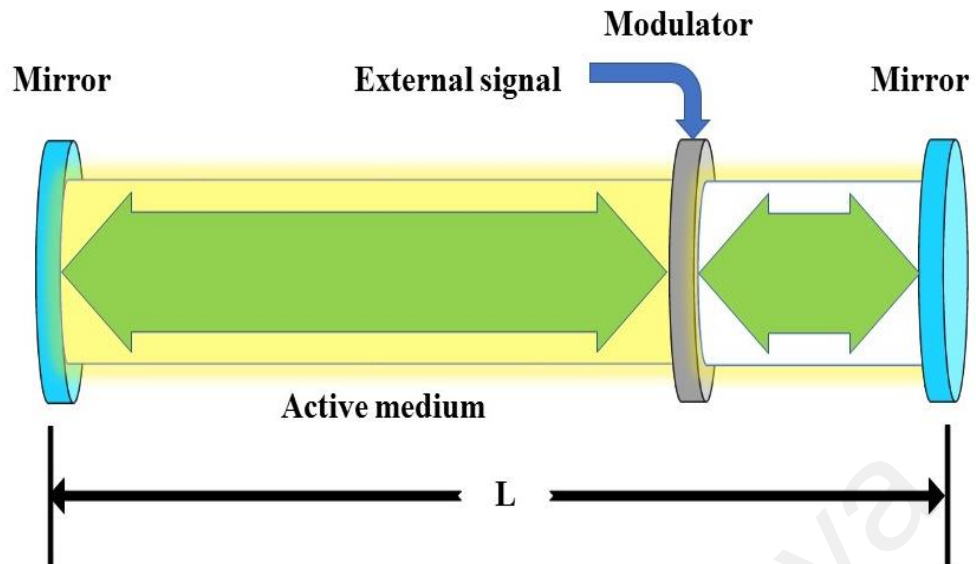


**Figure 2.8 The main components for active mode locked laser**

While in the passive techniques the need of modulator and external signal are eliminated. Rather, they generate mode locked pulses through the self-modulation of the light. This can be achieved using a device that is commonly known as a saturable absorber. The schematic of the passively mode locked laser is drawn in Figure 2.9. In general, saturable absorbers are the devices that have the ability to absorb the light and at a specific amount of intensity, it becomes saturated or transparent.

Therefore, when the saturable absorber is integrated inside the cavity, the low intensities of light will be attenuated while the high intensities are passed through the saturable absorber. As this process is repeated many times while the light is oscillating in the cavity, only the high intensities of light will be selectively amplified leading to the release of mode locking pulses. Passively mode locking techniques are highly preferable on the active techniques owing to the simplicity of the design, the cost effectiveness and furthermore, it can produce light with a much shorter pulse width that can be produced by the active techniques (Ngo, 2010).

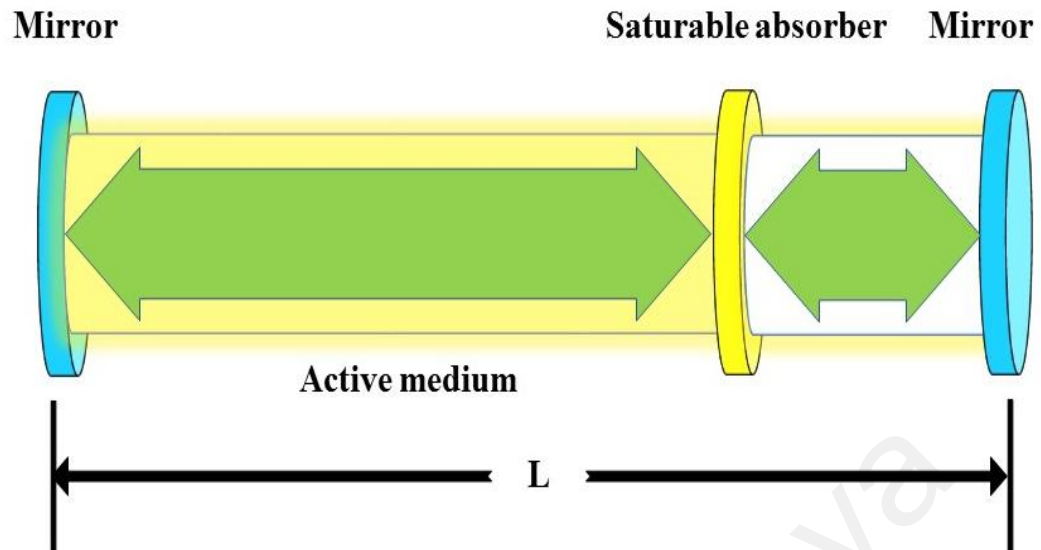


**Figure 2.9 The main comments of passively mode locking**

Many saturable absorbers have been investigated and reported for demonstrating mode locked lasers such as NPR [8, 9], SESAMs (Qingsong et al., 2017; X. Sun et al., 2017), NOLM (Cai et al., 2017; Zhong et al., 2010), CNT, TIs, TMDs, graphene, and BP. However, each of these SAs has got some limitations, as mentioned earlier in chapter one, which restrict its range of applications. Consequently, researchers being boosted to further investigate for new materials that can be used as an SA with better performance. In this report, I am proposing ZnO thin film as novel SA for demonstrating a mode locked EDFL to what it has from highly desirable optical properties that will be discussed in detail in the next section.

## 2.5 Saturable absorbers

Even though mode locking pulses can be released using many schemes, mode locking techniques using saturable absorbers are largely preferred because they terminate the requirement for the costly and complex optical modulators that limit the pulse duration. Saturable absorbers are those devices who have the ability to exhibit an intensity-dependent transmission which means that their ability to transmit light vary with the

amount of the light intensity that illuminates that device. In case of small amount of light subjected to the saturable absorber, all the light will be absorbed leaving zero transmission. While by increasing the amount of light, at one point the material will be fully saturated and turn to be transparent. Broadly, saturable absorbers can be classified into real SAs and artificial SAs. Real SAs are the materials that exhibit a nonlinear increase in the transmission with increasing light intensity while artificial SAs utilize the nonlinear effect to mimic the action of a real saturable absorber (R. I. Woodward & Kelleher, 2015). In this report, I am proposing zinc oxide (ZnO) thin film as real SA, therefore, my review will be restricted to real SAs only.

In fact, the evolution of the technology of saturable absorbers is increasing gradually with the evolution of lasers. The first Q-switched lasers based SAs were demonstrated in 1964 using a “reversibly bleachable” dye (Soffer, 1964) and a coloured glass filter (Bret & Gires, 1964). The year after, mode locked laser based SA was reported using rhodamine based organic dye. Then, last two decades the development of the passive fiber lasers are increased dramatically through the exploration of new generations of SAs. The historical evolution of the saturable absorber technologies is highlighted in Figure 2.10. In the early 1990s, the rapid development in the semiconductor technologies paved the way for the new type of saturable absorber which is a semiconductor saturable absorber mirror (SESAM) (Zirngibl et al., 1991). SESAMs have a controllable bandgap based on multiple quantum well structures (MQW) or quantum dot (QD) structures. Furthermore, by changing the type of the material and the geometry of the device, it can be designed to operate in the c-band that mainly used for the communication applications. Therefore, since that time, SESAMs have been utilized as a highly successful SAs in demonstrating both ultrafast mode locked fiber lasers and high energy Q-switched lasers (Qingsong et al., 2017; X. Sun et al., 2017). However, SESAMs got some limitations such as relatively expensive and complex fabrication process, low damage threshold, narrow operating

bandwidth and limited relaxation speed (M. H. M. Ahmed, 2015). Consequently, a new generation of SAs has to be explored in order to overcome that downside of SESAMs.

Then in the lately of 1990s a novel and very promising generation of SAs have started based on nanomaterials which got the advantages of the simpler fabrication process and faster recovery time than previous generations. Moreover, a much stronger quantum confinement will accrue by reducing the dimensionality of the SA (R. I. Woodward & Kelleher, 2015). In 1997 the first Zero dimensional (0D) nanomaterials were exploited in the generation of light pulses (Guerreiro et al., 1997). Then, during the last decade one dimensional (1D) carbon nanotube and two-dimensional (2D) graphene nanomaterials were explored as a novel promising saturable absorber because of their advantages of low cost, simple to fabricate, ultra-fast recovery time and operate in wide wavelength band (M. Ahmed et al., 2014; Z. Sun et al., 2009). However, it is complex to control the bandgap of the CNT which limit their operating range. While graphene has zero bandgap and its absorption co-efficiency is relatively low, consequently, restrict its range of applications. A few years ago, many other 2D materials have also been investigated and proposed as encouraging saturable absorbers in the construction of Q-switched and mode locked fiber lasers. Those 2D materials were extracted from different bulk materials such as transition metal dichalcogenides (TMDs), topological insulators (TIs) and black phosphorous (BP). To these days, TIs nanomaterials such as bismuth selenide ( $\text{Bi}_2\text{Se}_3$ ) (L. Gao et al., 2015), and bismuth telluride ( $\text{Bi}_2\text{Te}_3$ ) (Boguslawski et al., 2015); and TMDs nanomaterials such as tungsten disulphide ( $\text{WS}_2$ ) (Z. Sun et al., 2009), tungsten diselenide ( $\text{WSe}_2$ ) (Mao et al., 2016), molybdenum disulphide ( $\text{MoS}_2$ ) (M. Ahmed et al., 2016), and molybdenum diselenide ( $\text{MoSe}_2$ ) (Z. Luo et al., 2015) have been comprehensively reported as SAs for constructed fiber lasers in  $1\mu\text{m}$ ,  $1.5\mu\text{m}$  and  $2\mu\text{m}$  wavelength reigns.

On the other hand, transition metal oxides which are nonlinear optical materials that have been intensively investigated and widely used in the electrooptic applications over the past few decades due to their large optical nonlinearity and the advantages of good thermal and chemical stability in addition to mechanical strength. However, only few reports have been proposed transition metal oxides such as zinc oxide (ZnO) (Ahmad, Lee, Ismail, Ali, Reduan, Ruslan, & Harun, 2016; Ahmad, Lee, Ismail, Ali, Reduan, Ruslan, Ismail, et al., 2016; Ahmad, Salim, et al., 2016; Aziz et al., 2017), titanium dioxide (TiO<sub>2</sub>) (Ahmad, Reduan, et al., 2016) and Aluminum oxide (Al-Hayali et al., 2017) as SAs. Hence, more study is needed to utilize the valuable optical properties of the transition metal oxide nanomaterials for the pulse generation applications.

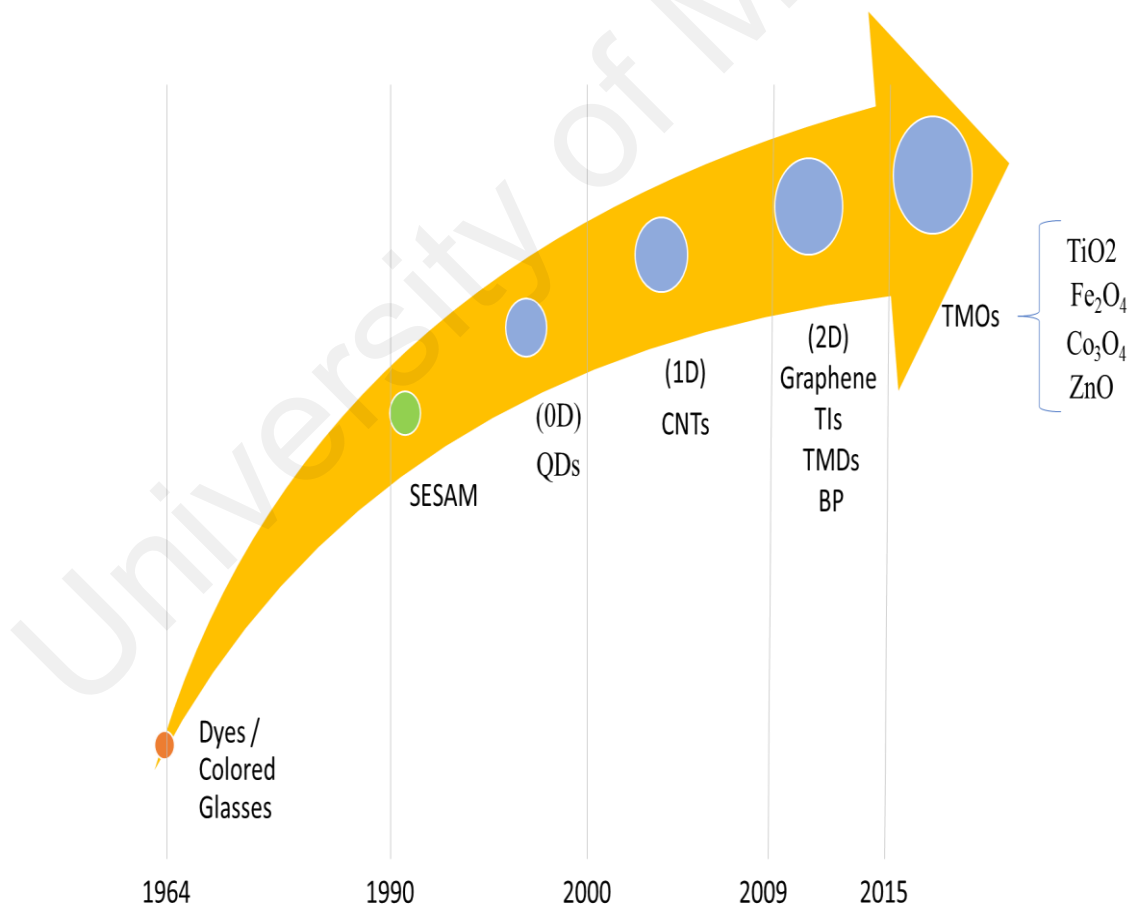


**Figure 2.10** The historical evolution of the saturable absorber technologies (the balls in blue color indicate the nanomaterials)

### 2.5.1 Zinc Oxide (ZnO)

In recent years, interest of transition metal oxides nanomaterial and nano sized semiconductor materials has been dramatically increased owing to their enormous desirable properties and applications in various areas such as chemistry, catalysts, biotechnology, photoelectron devices, environmental technology, sensors, information technology and highly functional and effective devices (Aneesh et al., 2007; Sangeetha et al., 2011; Wang, 2004). These nanomaterials have a wide bandgap between conduction and valence band and the large surface area which result in higher surface energy and consequently, it can show atom-like behaviors (Van Dijken et al., 2000). Therefore, a novel optical and electrical properties which are highly valuable in electrooptic applications can be obtained from these nanostructured materials. Moreover, metal nanoparticles are used in many biomedical applications to what it has from advantages such as self-cleansing, non-toxic and compatible with skin (Van Dijken et al., 2000).

The unique optical and electrical properties of nanoscale Zinc oxide (ZnO) have made it one of the best metal oxides that can be used in wide applications such as many industrial areas, solar cells, cosmetic industries, gas sensors, optoelectronics and photo catalyst (Bose & Barua, 1999). Furthermore, the broad chemistry and other favorable aspects of ZnO paved the way for many opportunities such as biocompatibility, wet chemical etching, radiation hardness and low power threshold for optical pumping (Sangeetha et al., 2011). All these properties of ZnO make it an ideal candidate for a variety of devices ranging from sensors through to ultra-violet laser diodes and nanotechnology-based devices such as displays.

In fact, the optical properties of ZnO are heavily influenced by the energy band structure and lattice dynamics. ZnO has direct band-gap of 3.4eV (Jagadish & Pearton, 2011) and exciton binding energy of 60 meV at room temperature (Bagnall et al., 1997).

While the lattice dynamics of ZnO is indicated in Figure 2.11. The figure shows a hexagonal lattice of ZnO crystallizes in the wurtzite (B4 type) structure at a pressure and temperature of the ambient. We can see that Zn ion is surrounded by tetrahedra of O ions, and vice-versa, therefore, the lattice can be characterized by two interconnecting sublattices of  $Zn^{2+}$  and  $O^{2-}$ . The polar symmetry which rises along the hexagonal axis due to the tetrahedral coordination is the responsible for many of ZnO properties such as spontaneous polarization and piezoelectricity. Additionally, this polarity is the key factor in etching, crystal growth and defect generation (Coleman & Jagadish, 2006).

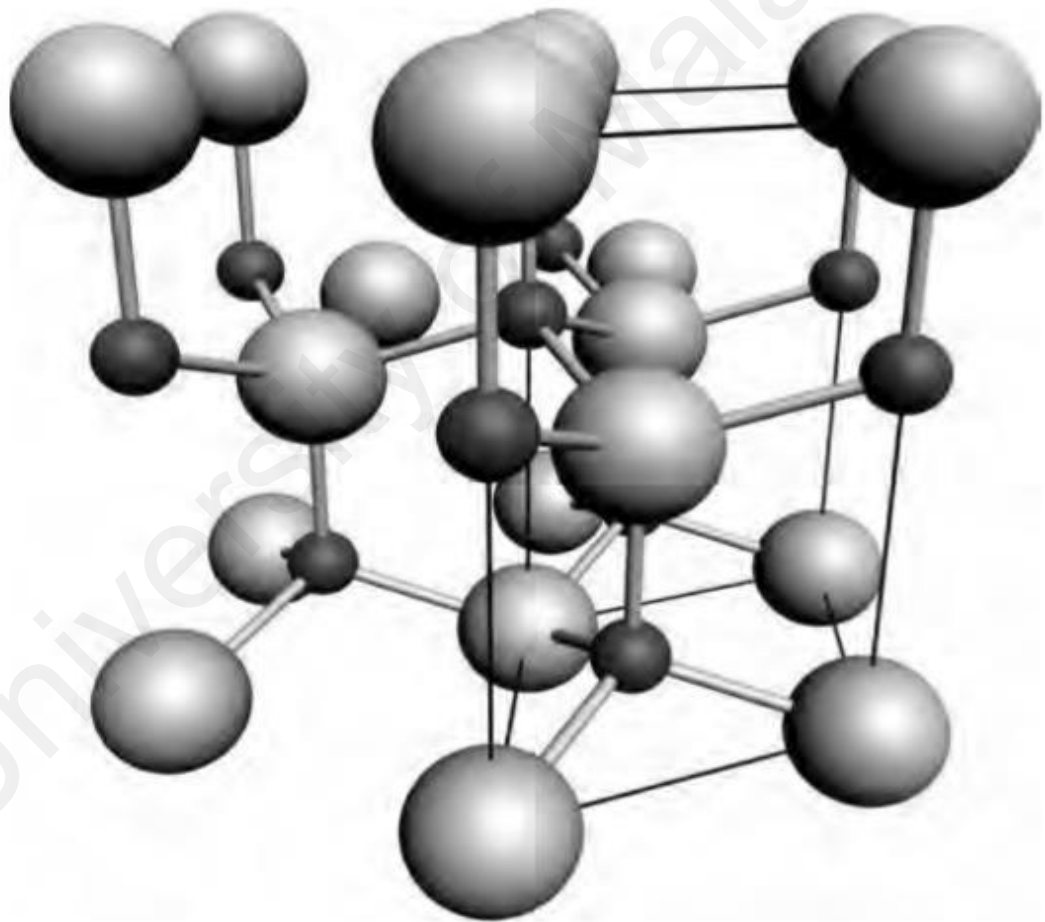


**Figure 2.11** The hexagonal wurtzite structure of ZnO. O atoms are shown as large white spheres, Zn atoms as smaller black spheres. One unit cell is outlined for clarity.(Coleman & Jagadish, 2006)

Usually, when the material has an ultrafast recovery time ( $\sim$ ps), wide band absorption, quite high damage threshold, appropriate modulation depth, low saturation intensity, simple fabrication process and economy, it is identified as an ideal saturable absorber for the fiber laser applications (Hasan et al., 2009). ZnO has high third-order nonlinear coefficient and it shows a recover time as short as 1–5 ps when examined via time-resolved second harmonic generation (Johnson et al., 2004). While the optical nonlinearities of ZnO have been investigated using the single-beam z-scan method. The results of this investigation revealed that the nonlinear absorption of ZnO is due to the two-photon resonance at the band edge and exciton energy level while the optical nonlinearity is induced by the free carrier (Ja-Hon Lin et al., 2005). Another investigation of the optical nonlinearity of ZnO using the same method showed a switchover from Reverse Saturable Absorption to Saturable Absorption which is an interesting characteristic for ultrafast optical switching applications such as Q-switched and mode locked fiber laser (Haripadmam et al., 2014). Furthermore, ZnO has high sustainability to damage threshold, simple fabrication process and it is environment friendly (Ahmad, Lee, Ismail, Ali, Reduan, Ruslan, Ismail, et al., 2016; Jamdagni et al., 2016). Despite all these highly desirable properties of ZnO, only recently it has been proposed as an ideal saturable absorber for fiber laser applications. To date, Q-switched fiber lasers have been constructed and reported using ZnO as a SA (Ahmad, Lee, Ismail, Ali, Reduan, Ruslan, & Harun, 2016; Ahmad, Lee, Ismail, Ali, Reduan, Ruslan, Ismail, et al., 2016; Ahmad, Salim, et al., 2016; Aziz et al., 2017). However, to the best of my knowledge, no mode locked EDFL using ZnO as SA has not been reported yet.



## **CHAPTER 3: NANOSECOND MODE-LOCKED ERBIUM DOPED FIBER LASER BASED ON ZINC OXIDE THIN FILM AS A SATURABLE ABSORBER**

### **3.1 Introduction**

Since been introduced, mode locked Erbium-doped fiber lasers (EDFLs) have found their place in many applications begin from basic research to very complex and accurate devices which are used in highly sensitive applications with extremely low tolerance of error including micromachining, telecommunication, ophthalmology, laser surgeries and optical sensing (Dausinger & Lichtner, 2004; Fermann et al., 2002; Osellame et al., 2012). Nanosecond mode locked pulsed lasers have not been adequately investigated even though they got the advantages of high pulse energy and average power scaling in addition to the pulses produced from such lasers are usually giant-chirped and have large duration and low peak power (Ismail et al., 2012; Xia et al., 2014).

Owing to these advantages of the nanosecond pulsed lasers, they have been utilized as a pump power source for generating a mid-IR supercontinuum (R. Woodward et al., 2015) and as a seed oscillator for chirped-pulse amplification systems (Renninger et al., 2008). During last decade, nanosecond passively EDFLs have been constructed and reported using different saturable absorbers (SAs) such as semiconductor SA mirror (SESAM) (Chen et al., 2009), NPR (Mao et al., 2010), carbon nanotubes (CNT) (Ismail et al., 2012) and graphene (Xia et al., 2014; Xu et al., 2012). However, each of these SAs has some limitations as mentioned earlier.

Recently, ZnO has been seen as an ideal SA candidate due to its high sustainability to damage threshold, high nonlinear optical response, simple fabrication process, fast recovery time and environment friendly (Ahmad, Lee, Ismail, Ali, Reduan, Ruslan, Ismail, et al., 2016; Jamdagni et al., 2016). To date, Q-switched fiber lasers have been constructed and reported using ZnO as an SA [28, 30-32]. However, mode locked EDFL

using ZnO as SA has not been reported yet. In this chapter, at first, ZnO is fabricated into a thin film by mixing the seeding solution with the PVA.

Then, the fabricated ZnO thin film SA has been characterized using Field Emission Scanning Electron Microscopy (FESEM), Raman spectrum, white light source and balance twin detector technique. Finally, a small piece of the fabricated ZnO thin film is used to experimentally demonstrate a nanosecond mode locked EDFL for the first time. The central wavelength of the laser is measured to be 1558.34 nm and the repetition rate and pulse width are 993 kHz 400 ns, respectively. The maximum output energy of the proposed laser is calculated to be approximately 11.6 nJ at a pump power of 142 mW.

### **3.2 The Fabrication of Zinc Oxide Thin Film**

The fabrication process of ZnO-SA is illustrated in Figure 3.1. At first, to prepare the ZnO seeding solution, 1 mM of zinc acetate dehydrate [ $\text{Zn}(\text{O}_2\text{CCH}_3)_2 \cdot 2\text{H}_2\text{O}$ , Merck] dissolved into 60 ml of ethanol at 60 °C for 30 minutes followed by cooling for 10 minutes.

After cooling, 60 ml of fresh ethanol were added to zinc acetate solution and 1 mM of sodium hydroxide [NaOH, Merck] was added 1 drop/s with aid of stirring. Then the seeding solution was placed in the water bath for 3 hours at 60 °C. After that, the ZnO thin film was fabricates by mixing the seeding solution into the PVA solution and stirred for 2 hours. Finally, the ZnO with PVA solution was slowly poured into a petri dish and dry at the ambient temperature for 3 days.

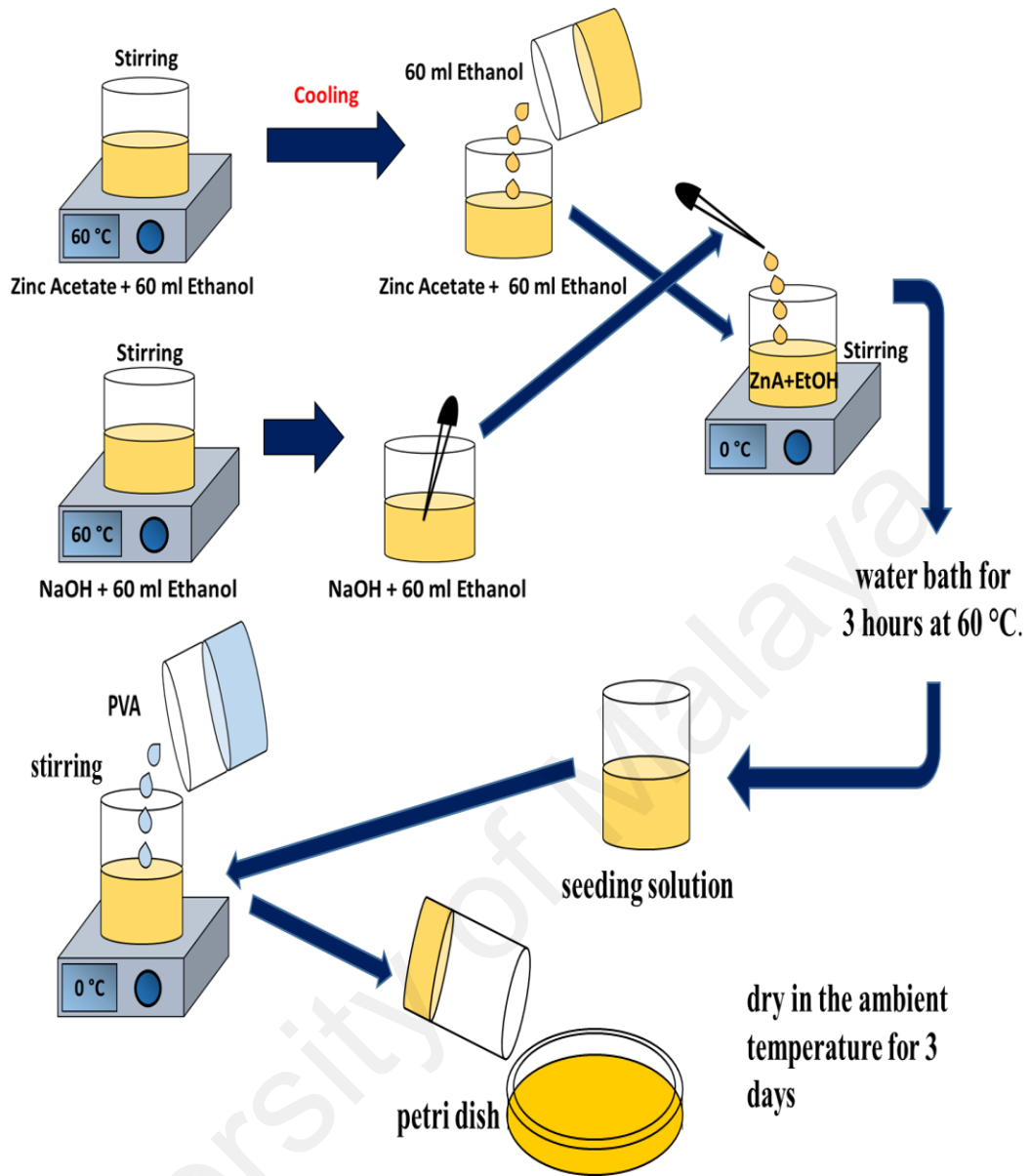


**Figure 3.1 Fabrication process of ZnO thin film saturable absorber**

### 3.3 Characterization of ZnO thin film

After the fabrication of the ZnO thin film, it is very important to characterize the fabricated thin film in order to verify the shape and the purity of the proposed nanomaterial. Furthermore, it is essential to measure the linear and nonlinear absorption of the nanomaterial within the operation wavelength range of the laser to prove their ability to absorb the light and function as an SA. The fabricated ZnO thin film is characterized using the following methods:

### 3.3.1 Field emission scanning electron microscopy (FESEM)

Figure 3.2 shows FESEM image of ZnO-PVA thin film, which displays an existence of the uniform layer with few particles in size between 0.31 to 1.77  $\mu\text{m}$ . This film shows bending on the surface due to the drying of the thin film as shown in the insert figure in high magnification. The thickness of ZnO-PVA film was measured to be around 50  $\mu\text{m}$ .

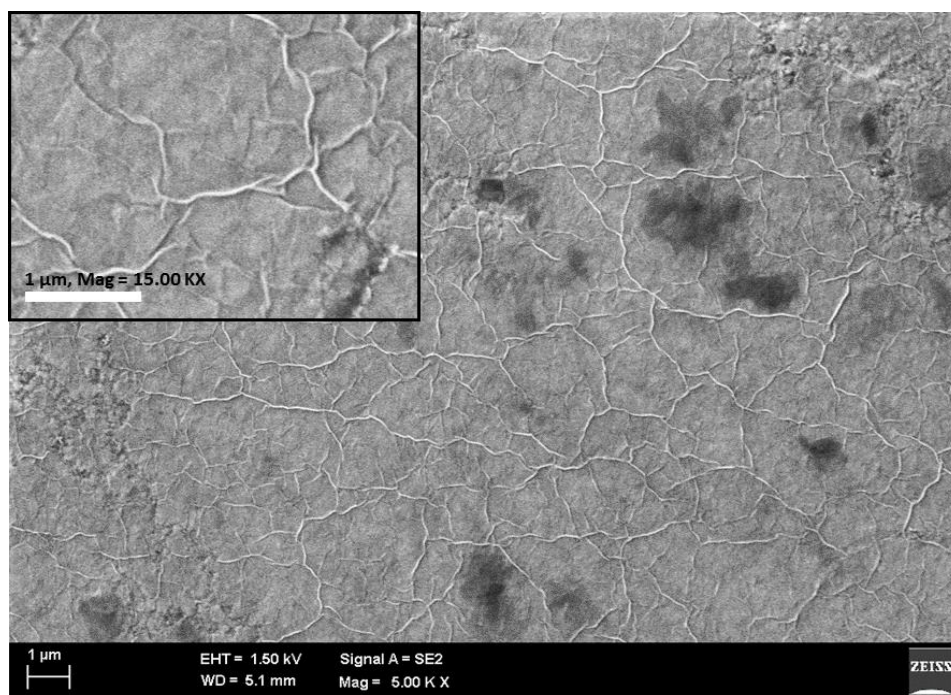


**Figure 3.2 FESEM images. Insert shows a high magnification of the image**

### 3.3.2 Raman spectrum

The micro-Raman scattering spectra of the ZnO: PVA thin film was determined by using excitation wavelength, laser power, and exposure time were about 514 nm, 1 mW, and 30 s, respectively. Raman scattering spectrum of ZnO embedded in PVA is shown in Figure 3.3 in range of 200-700  $\text{cm}^{-1}$ . The optical phonons of ZnO in Raman spectrum consist of polar and non-polar modes. The polar modes are  $A_1$  and  $E_1$  modes and both of them are split out into transverse optical (TO) and longitudinal optical (LO) modes. On the other hand, the non-polar modes are appeared as high and low modes and referenced as  $E_{2h}$  and  $E_{2l}$  modes, respectively. The appearance peaks in the spectrum at around 225.1, 368.8, 416.3, 481.7, 601 and 637  $\text{cm}^{-1}$  are corresponding to  $2E_{2l}$ ,  $A_1(\text{TO})$ ,  $E_1(\text{TO})$ ,  $E_{2h}$ ,

$A_1(LO)$  and  $E_1(LO)$ , respectively (Das & Mondal, 2014; Montenegro et al., 2013; Sharma et al., 2013). The insert image of the figure shows a PVA Raman shift in the range of  $1500-3000\text{ cm}^{-1}$ . At higher Raman shift, the peaks appeared at around  $1674.6$  and  $2930.1\text{ cm}^{-1}$  indicating to PVA phonon modes (Popa et al., 2010), as shown in the inset Figure 3.3.

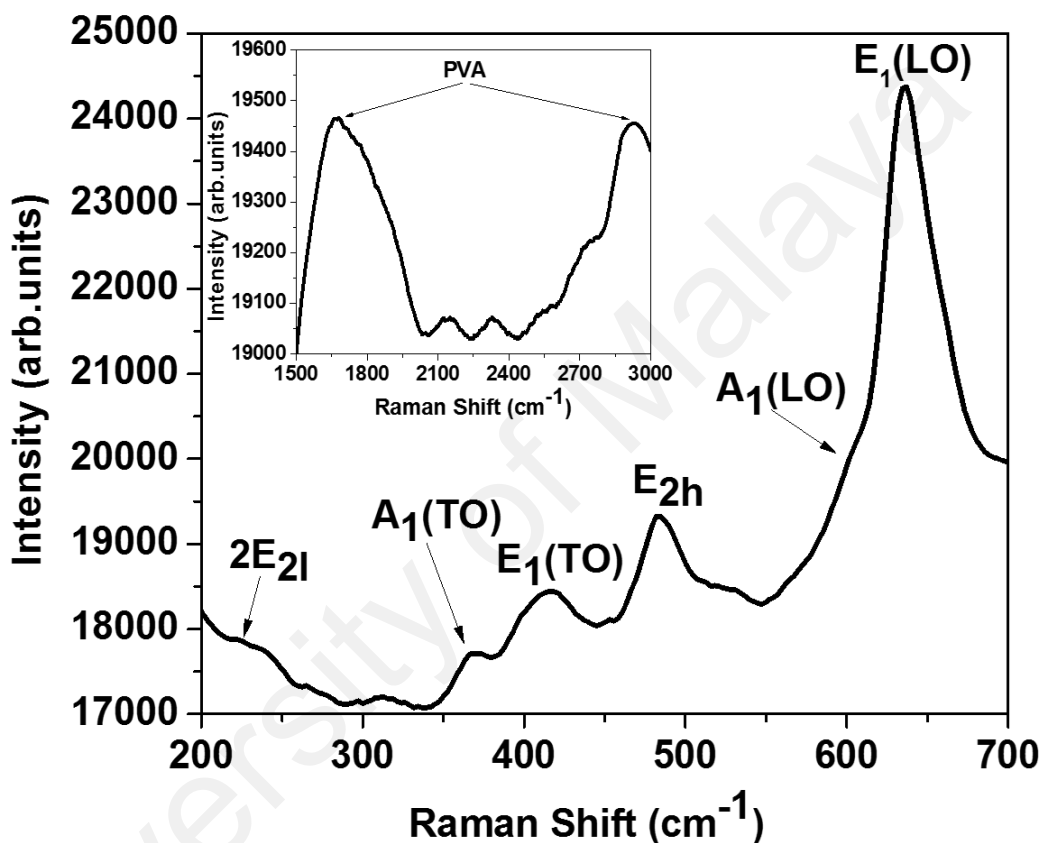
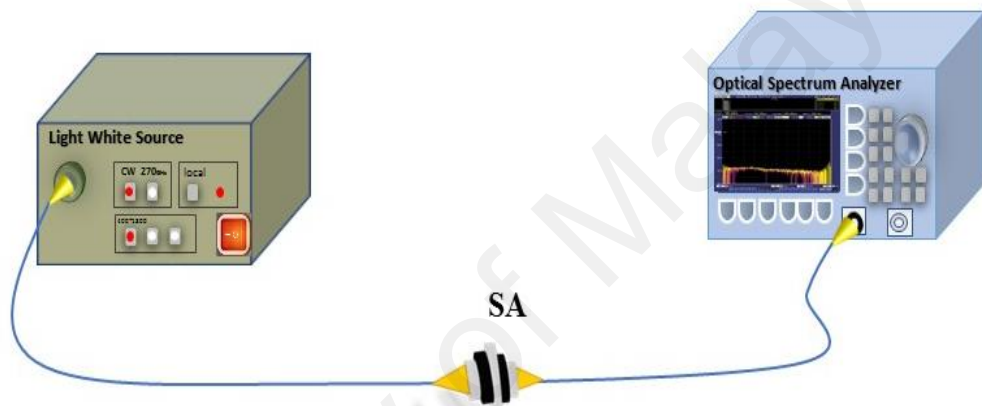


Figure 3.3 Raman spectrum of ZnO-PVA

### 3.3.3 Linear optical absorption

The white light source is used to investigate the linear absorption of the produced SA. The configuration of the experimental setup is shown in Figure 3.4. At first, the white light source is set on the CW mode of operation within the range of  $400\sim 1800\text{ nm}$ . Then, without inserting the ZnO-SA, the output spectrum is recorded as a reference. Then, the ZnO-SA is integrated between the white light source and the optical spectrum analyzer. Again, the output spectrum is recorded which represent the transmitted signal in this case.

After that, the absorption spectrum of the ZnO based SA is calculated as shown in Figure 3.5 by subtracting the transmitted spectrum from the reference signal. As indicated in Figure 3.5, the ZnO-SA shows an absorption ranging from 1000 nm to 1600 nm. It can be seen that the absorption spectrum starts at almost 5 dB and gradually decrease until 1250 nm, and then become almost linear at around 3.5 dB. The highlighted area in Figure 3.5 indicates the area of interest for this work and shows that the absorption in this region is mostly linear.



**Figure 3.4 The configuration of the linear absorption experiments**

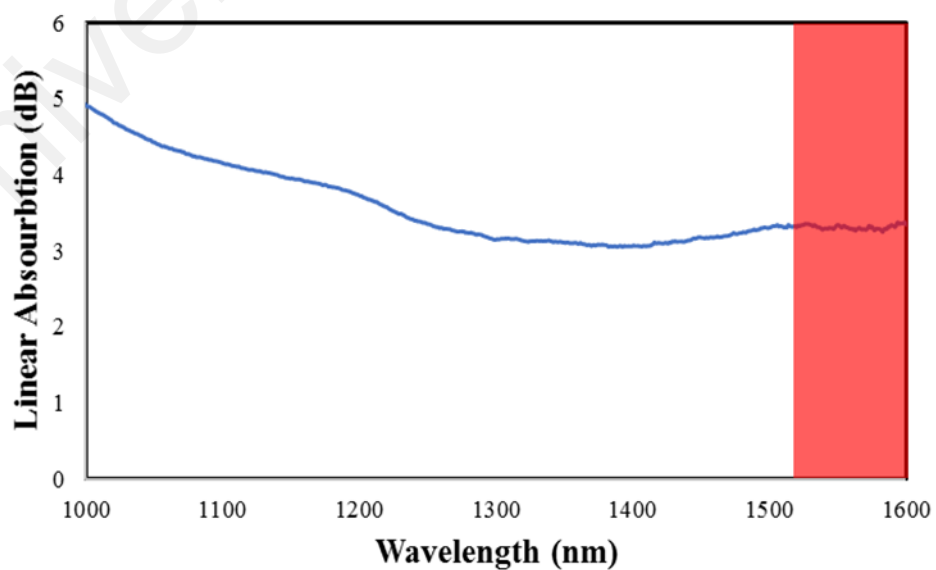


**Figure 3.5 Linear absorption spectrum of the ZnO based SA**

### 3.3.4 Nonlinear optical absorption

With the aim of the investigation of the nonlinear optical absorption of the proposed SA, a balance twin detector technique has been demonstrated as shown in Figure 3.6. Given that, the optical absorption range of the proposed ZnO-SA is 1000 up to 1600 nm after it is being illuminated by a white light source (Ahmad, Lee, Ismail, Ali, Reduan, Ruslan, Ismail, et al., 2016), we have used a 1550 nm homemade mode locked fiber laser to investigate the nonlinear absorption of the proposed SA. The repetition rate and the pulse width of the homemade mode locked source were 1 MHz and pulse width of 4.14 ps, respectively. As drawn in the figure, a commercial erbium doped fiber amplifier (EDFA) with low dispersion has been directly connected to the mode locked source for the purpose of amplifying the output power to a level adequate to fully saturate the ZnO-SA. Furthermore, a variable optical attenuator (VOA) is used to control the output power of the EDFA and vary it within a desirable range enough to estimate the modulation depth of the ZnO-SA. Afterward, a 3dB coupler is integrated after the VOA for the need of simultaneously measuring the output power after it basing through the SA and directly without SA to calculate the absorption of the SA. Finally, by using the readings taken from both the power meters which were connected to both ends of the 3dB coupler, the modulation depth is being estimated to be around 5% and the saturation intensity was 60 MW/cm<sup>2</sup> as shown in Figure 3.7.

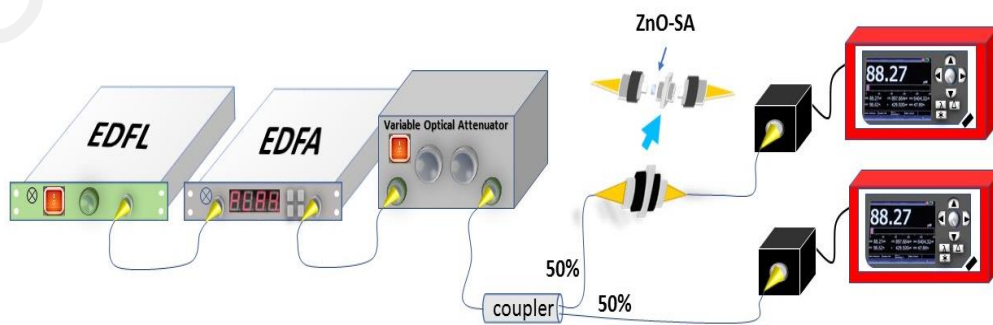


**Figure 3.6** The setup of the dual-detector technique

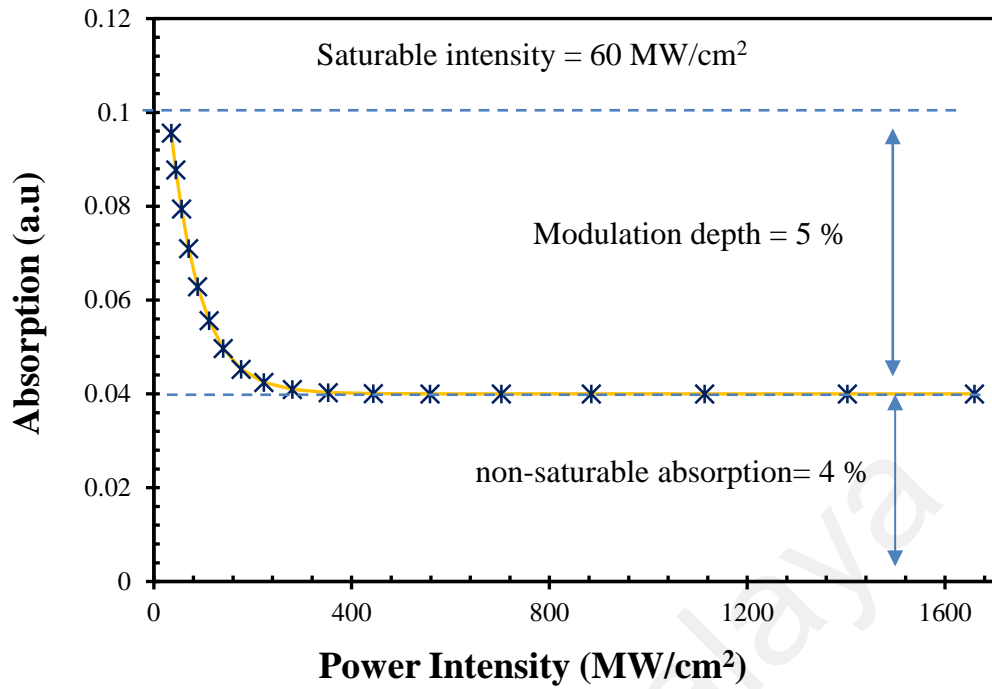


**Figure 3.7 Nonlinear absorption of the ZnO SA**

### 3.4 Experimental setup

The nanosecond mode locked EDFL's configuration has been drawn as shown in Figure 3.8. First, a laser diode (LD) is used as a pump source with a continuous output of 980 nm and it is being forwardly pumped the gain medium which is a 2.8 m erbium doped fiber (EDF) through the use of 980/1550 nm wavelength division multiplexer (WDM). At 980nm, the absorption of the erbium ions in the EDF is 23 dB/m, whereas its group velocity dispersion (GVD), the numerical aperture (NA), and the core and cladding diameters are 27.6 ps<sup>2</sup>/ km, 0.16, 4μm and 125μm, respectively.

Then, a polarization insensitive isolator is integrated directly after the EDF to the aim of the avoidance of the loss and the probable damage to the SA or LD caused by the back reflection of the light. So, its main function is to ensure the unidirectionality of the light inside the laser's optical resonator. At this point, the laser's optical resonator has been formed by using an 80/20 coupler where the majority of the light returns to the cavity



through WDM for the purpose of the amplification, and the remaining part of the light is being taken to the output.

Simply, the SA is constructed by sticking a small piece of the fabricated ZnO-SA with size around 1 mm diameter onto a clean ferrule connector using a matching index gel and then mated with another clean ferrule connector. The formed SA is then inserted inside the laser cavity as indicated in Figure 3.8. Furthermore, an extra 195 m single mode fiber (SMF-28) with GVD of  $-21.7 \text{ ps}^2/\text{km}$  is added to the cavity to increase its nonlinearity and dispersion, consequently promote the mode locking action. Therefore, the total length of the cavity becomes around 201.5 m where all from SMF-28 except the EDF length. Finally, a 3-dB coupler is used at the output in order to simultaneously view the output spectra and the oscilloscope (OSC) trace of the nanosecond mode locked EDFL. The cavity operates in anomalous fiber dispersion of  $-4.23 \text{ ps}^2$ .

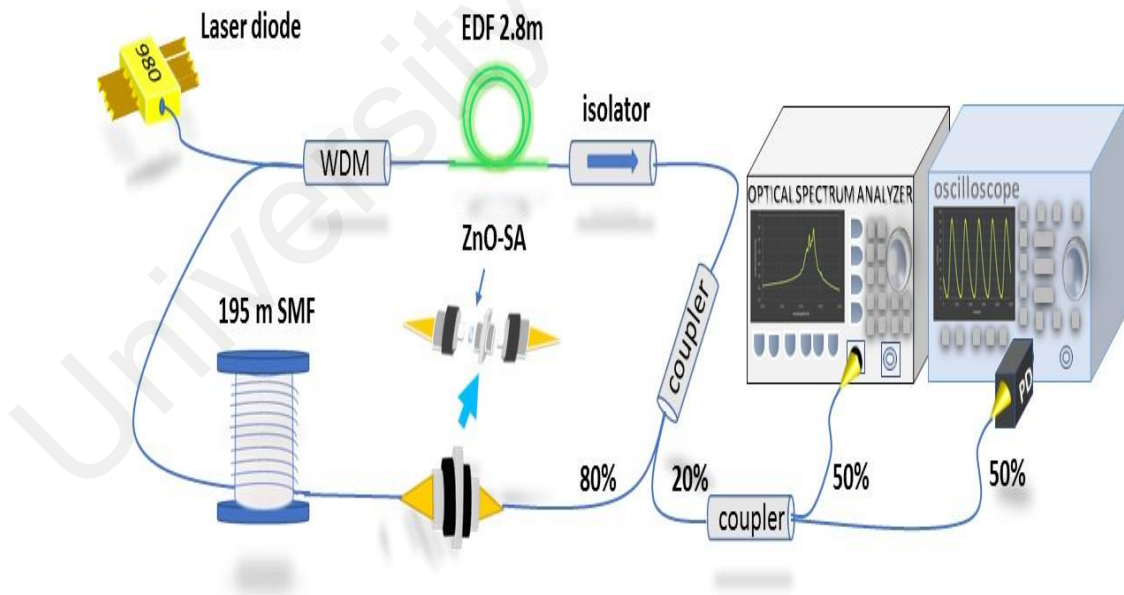


**Figure 3.8** Experimental setup of the proposed mode locked EDFL

### 3.5 Results and Discussion

In this section, the characteristics of the proposed nanosecond mode locked EDFL have been presented and discussed comprehensively. At a relatively low pump power of 45.5 mW, a stable self-started nanosecond mode locking pulses were realized without any Q-switching instabilities. The optical spectrum of the laser output is shown in Figure 3.9. As shown in the figure, a wide spectrum is observed which conforms the mode locking operation of the proposed laser. The central wavelength is measured to be 1558.34 nm at the maximum pump power of 142 mW while the 3-dB spectral bandwidth is 0.2 nm. The mode locking operation of the proposed laser is further conformed by observing the pulse train on the OSC as shown in Figure 3.10 (a). Where a uniform pulse train has been realized with a constant fundamental repetition rate of 993 kHz even though the pump power is being changed from the threshold value of the mode locked to the maximum available value of 142 mW. The fixed repetition rate is confirmed the essential property of the mode locking process. The pulse period is measured to be around 1  $\mu$ s while the pulse width is 400ns as indicated in Figure 3.10 (b). Furthermore, the measured repetition rate is verified with the calculated value based on the total cavity length.

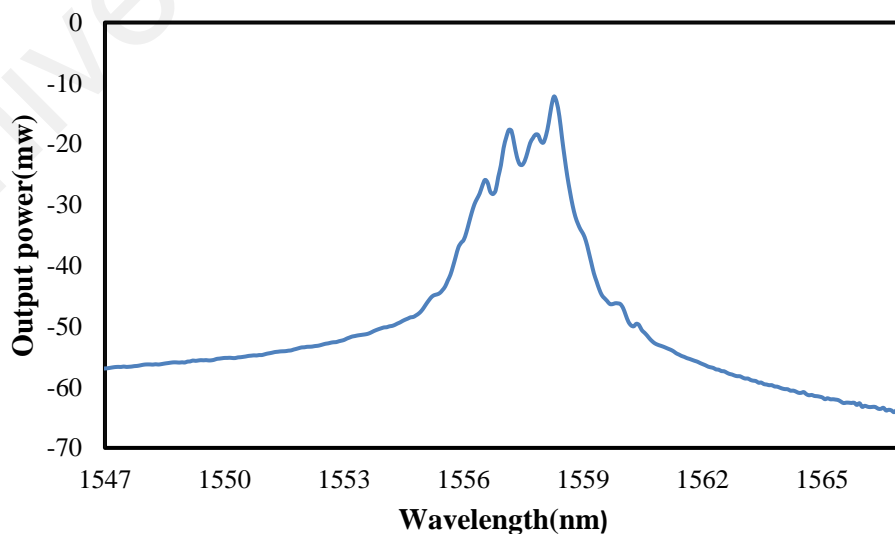


**Figure 3.9 Output spectrum of mode-locked EDFL at pump power of 142 mW**

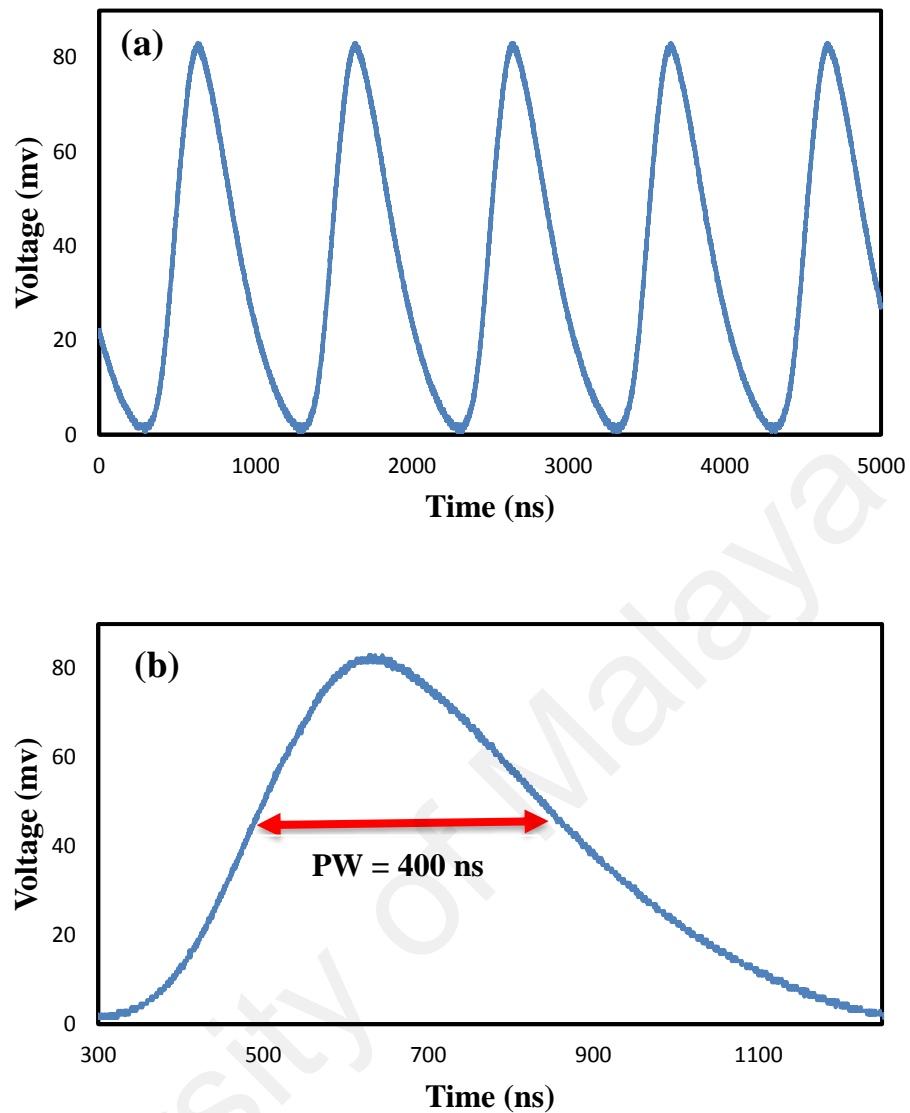


**Figure 3.10 (a) The oscilloscope trace of the mode-locked EDFL at pump power of 142 mW (b) single envelope of the pulse**

After the output of the laser is being characterized in the time domain, we have investigated the frequency domain as well as to the aim of the verification of the signal stability. The radio frequency (RF) spectrum of the proposed mode locked EDFL based ZnO-SA is depicted in Figure 3.11. The RF spectrum shows a very good stability around 64 dB signal to noise ratio (SNR) for the mode locked pulse at the fundamental repetition rate with span and a resolution bandwidth of 7000 kHz and 30 kHz, respectively. Furthermore, when the ZnO-SA is removed from the cavity the mode locked pulse has disappeared which ensure the role of the SA to generate mode locked pulse.

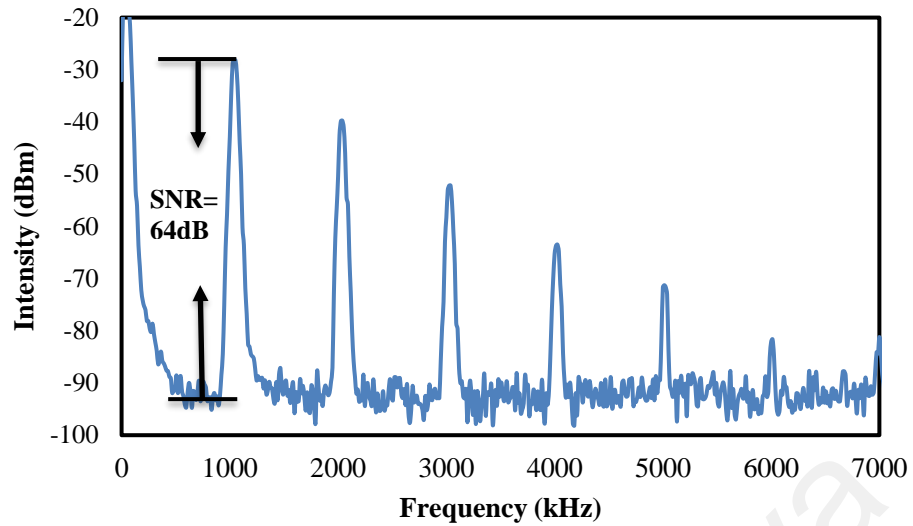


**Figure 3.11 RF spectrum of the mode locked at 142 mW**

Finally, the average output power and pulse energy of the mode locked output have been characterized at various pump powers as illustrated in Figure 3.12. The linearity relationship of both the average power and the pulse energy with the pump power is obvious as shown in Figure 3.12. Then, the maximum output power at the maximum available pump power of 142 mW is measured to be 11.54 mW. While the peak power and pulse energy have been estimated to be 27.3 mW and 11.6 nJ, respectively.

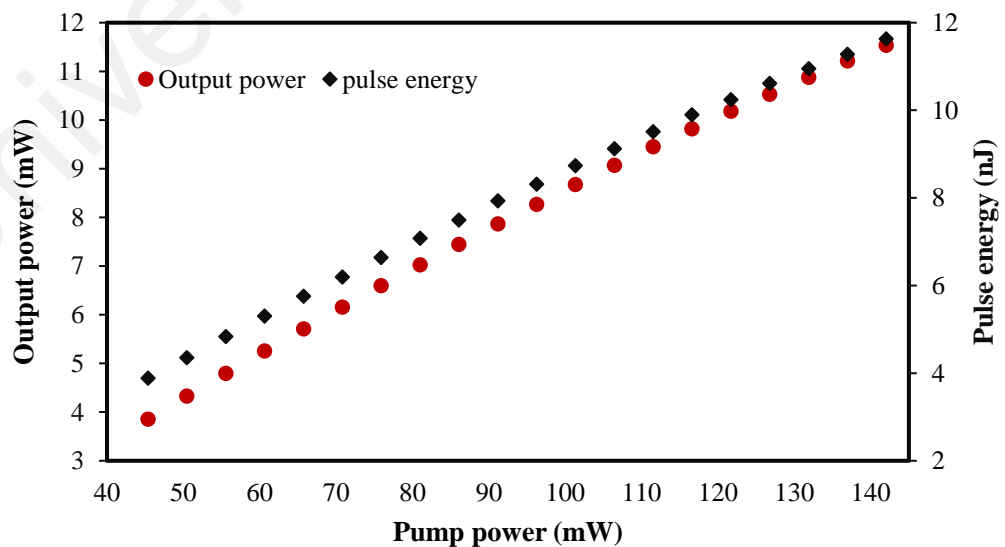


**Figure 3.12 Output power and pulse energy as a function of 980nm pump power.**

### 3.6 Summary

Despite nanosecond mode locked fiber lasers offer the advantages of high pulse energy and average output power with large duration, they being rarely constructed and reported in the literature. In this chapter, ZnO thin film SA was firstly fabricated and characterized using FESEM, Raman spectrum, white light source and balance twin detector technique. Then, a passively nanosecond mode locked EDFL has been constructed based on the fabricated ZnO-SA for the first time. After the fabricated ZnO thin film was integrated inside the ring cavity of the EDFL as an SA, self-started mode locked pulses of 400 ns pulse width was realized at a relatively low pump power of 45.4 mW. The central wavelength and the fundamental repetition rate were measured to be 1558.43 nm and 993 kHz, respectively. The pulse energy and the peak power of the laser were 11.6 nJ and 27.3 mW respectively at the maximum pump power of 142 mW. This shows that the ZnO can be a promising candidate for SA in generating nanosecond mode locked pulses train.

## **CHAPTER 4: PICOSECONDS MODE-LOCKED ERBIUM DOPED FIBER LASER BASED ON ZINC OXIDE THIN FILM AS SATURABLE ABSORBER**

### **4.1 Introduction**

In the previous chapter, the fabricated ZnO-SA was integrated into a 201.5 m long ring laser cavity. The repetition rate of the mode locked pulses was obtained at 993 kHz, which agreed with the cavity length and the pulse width was 400 ns. In this chapter, the repetition rate is increased around three times greater than the first experiment by using different cavity with a shorter length of 61.5 m. This relationship between the cavity length and the repetition rate is one of the mode locking properties. Where the repetition rate is reverse proportional to the cavity length based on the equation (2.1). Hence, the shorter the cavity length, the larger locking bandwidth that laser can give (Z. Ahmed et al., 1992). Furthermore, in this experiment, pulse width as short as 1.76 ps is achieved. This mode locked picoseconds pulses with high peak power and high repetition rate are very attractive to various laser applications such as microelectronics and semiconductor industries (Patel & Bovatsek, 2007). That is owing to the very clean and accurate removal of material that can be achieved by the picoseconds pulse duration with high peak power, in addition, to minimizing the thermal damage. While the high repetition rate increases the processing speed. Moreover, mode locked EDFLs of high repetition rates have a considerable interest in the optoelectronic applications that required high speed. As a result, those lasers have been extensively explored in a wide range of applications such as high-speed optical communication systems, optical frequency metrology, ultrafast data processing and high-speed optical sensing (Arahira et al., 1996).

On the other hand, L-band recently becomes very interesting band due to the increase in the demand for more wavelengths to expand the transmission capacity in the optical communication system. Also, at this band silica fibers have the slowest losses which consequently will increase the transmission distance.

Here, the previously fabricated ZnO thin film (as described in the previous chapter) is used to construct another mode locked EDFL operating in picosecond regime. The laser operates at a repetition rate of 3.26 MHz with a central wavelength of 1599.5 nm in the L-band region. The maximum output power was 6.91 mW at a pump power of 159 mW. The proposed laser can be seen as a promising light source in the optical communication system.

## 4.2 Experimental setup

The configuration of the proposed mode locked EDFL with ZnO-SA, which was optimized for picosecond pulse generation, is shown in Figure 4.1. The pump source of the laser is a 980-nm LD which being connected to 980/1550 nm WDM. A 3 m EDF was used as a gain medium with core and cladding diameters of 4  $\mu\text{m}$  and 125  $\mu\text{m}$ , NA of 0.16, erbium ion absorption of 23 dB/m at 980 nm and GVD of 27.6  $\text{ps}^2/\text{km}$ . In order to ensure the unidirectionality of the light in the cavity which is essential to avoid the loss due to the back reflection as well as to reduce the probability of the SA and LD to be damaged, a polarization insensitive isolator was placed after the EDF.

A small piece of the fabricated ZnO-SA was sandwiched between two FC/PC fiber connectors and directly inserted inside the cavity after the isolator. A 90/10 coupler was used to provide 90% of the light feedback to the cavity via the 1550 nm port of the WDM passing through a 50 m-long standard SMF-28 with GVD of -21.7  $\text{ps}^2/\text{km}$  to increase the non-linearity and dispersion in the cavity. The other 10 % extract to the output, which connected to An AQ6373 optical spectrum analyzer (OSA) with 0.07 nm resolution and an OSC via a fast photodetector. Also, an auto-correlator is used to measure pulse duration. All the components are made of SMF-28 or pigtailed with SMF-28 with a length of 8.5 m. The total cavity length is 61.5 m, which operates in anomalous fiber dispersion of -1.187  $\text{ps}^2$ .

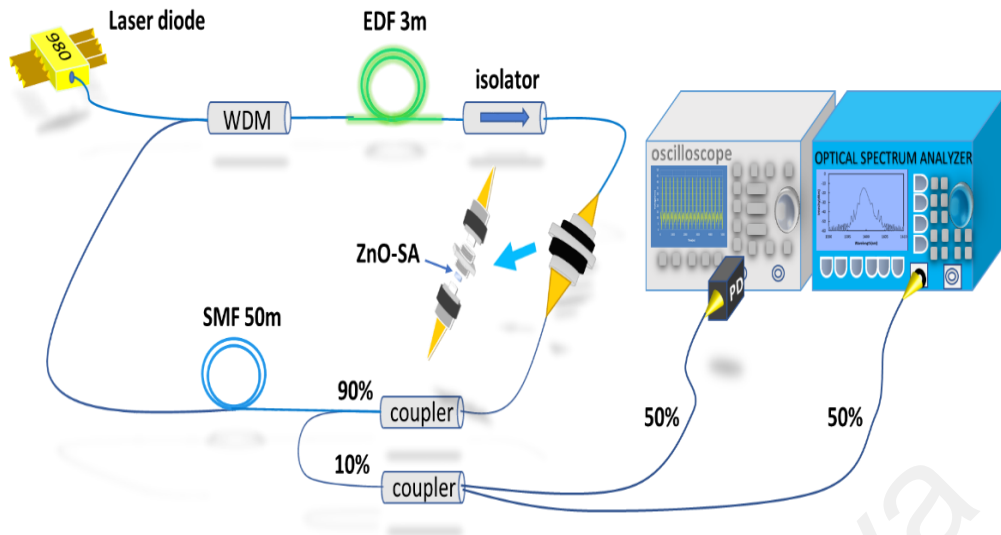


**Figure 4.1 Experimental setup of the proposed mode locked EDFL for picosecond pulse generation.**

### 4.3 Mode-locking performance

After ZnO-SA being integrated into the cavity and the pump power from 980nm laser diode being increased slightly, continuous lasing is observed at a low pump power of 20 mW showing the low insertion loss of the ZnO-SA. When the pump power is increased to 42 mW, self- started mode locked pulse is being formed. The mode locked output pulse was maintained stable and ZnO-SA was functioning properly without thermal damage as the pump power reached the maximum value of 159 mW.

The output spectra of the mode locked EDFL is shown in Figure 4.2, which is centered at 1599.5 nm L-band with a 3dB spectral bandwidth of 1.12 nm. The OSC trace of the mode-locked EDFL at 159 mW is illustrated in Figure 4.3. As shown in the figure, a uniform pulse train is being generated with a pulse period around 306 ns and fundamental repetition rate of 3.26 MHz. The measured value of the repetition rate is comparable to the calculated value by the length of the cavity and the refractive indices of the different fibers that form the cavity.



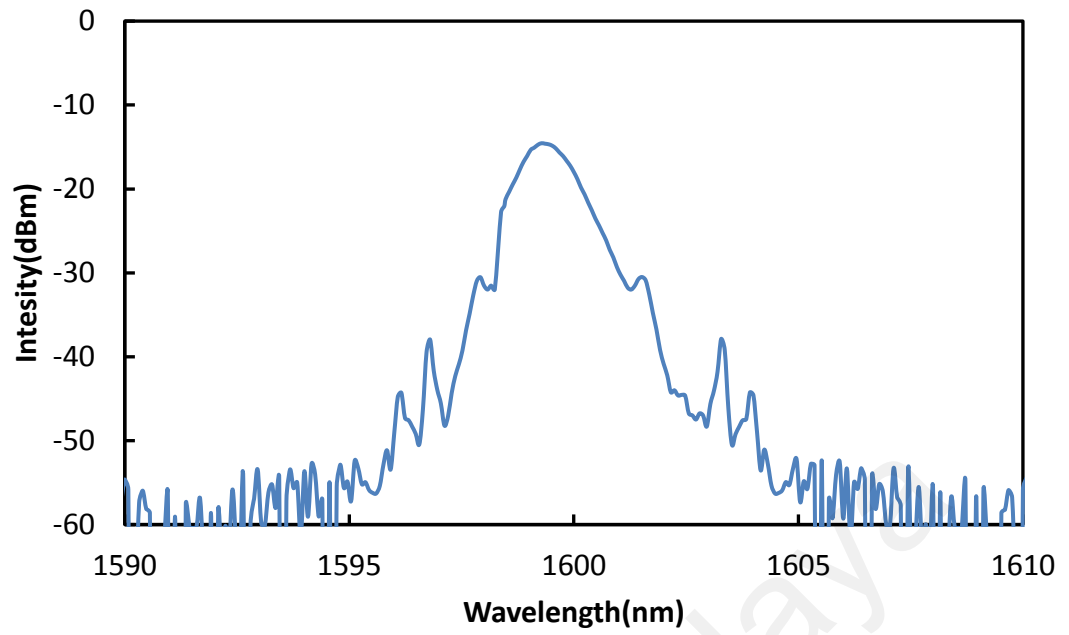


**Figure 4.2 Output spectrum of mode-locked EDFL at a pump power of 159 mW.**

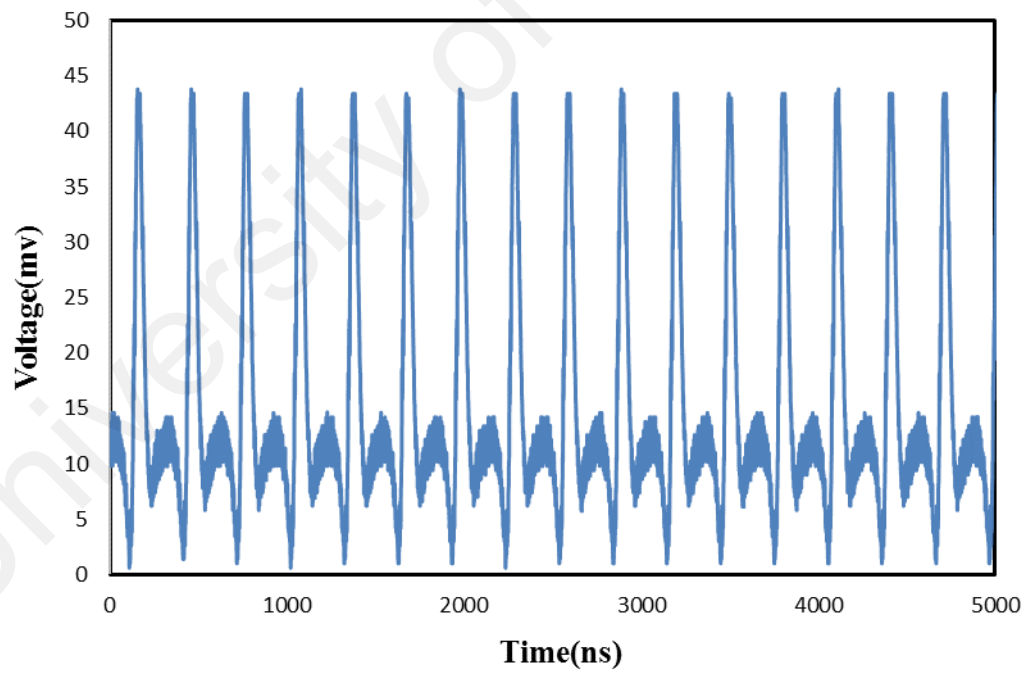


**Figure 4.3 The oscilloscope trace of the mode-locked EDFL at a pump power of 159 mW.**

Due to the scale limitation of the oscilloscope, autocorrelator was used to accurately measure the pulse width of the output pulses. The autocorrelation trace of the mode-locked EDFL is shown in Figure 4.4. As indicated in the figure, the measured pulse duration and the  $\text{sech}^2$  pulse profile are in line, where the pulse duration at the full width half maximum (FWHM) is measured to be 1.76 ps. The stability of the output pulses of the laser has been investigated by characterizing the RF spectrum which is shown in Figure 4.5. The RF spectrum was recorded with 100 MHz span and 30 kHz resolution bandwidth. The stability of the pulse has been conformed with a relatively high SNR of 54 dB at the fundamental frequency of 3.26 MHz. Finally, at various pump powers, we have investigated the average output power and the pulse energy of the mode locked EDFL based ZnO-SA as indicated in Figure 4.6. A linearly increasing of the average output power and the pulse energy is observed as the pump power increase. Furthermore, the pulse energy and peak power of the laser have been estimated at the maximum pump power of 159 mW and average output power of 6.9 mW, where they found to be 2.13 nJ and 1.14 kW, respectively.

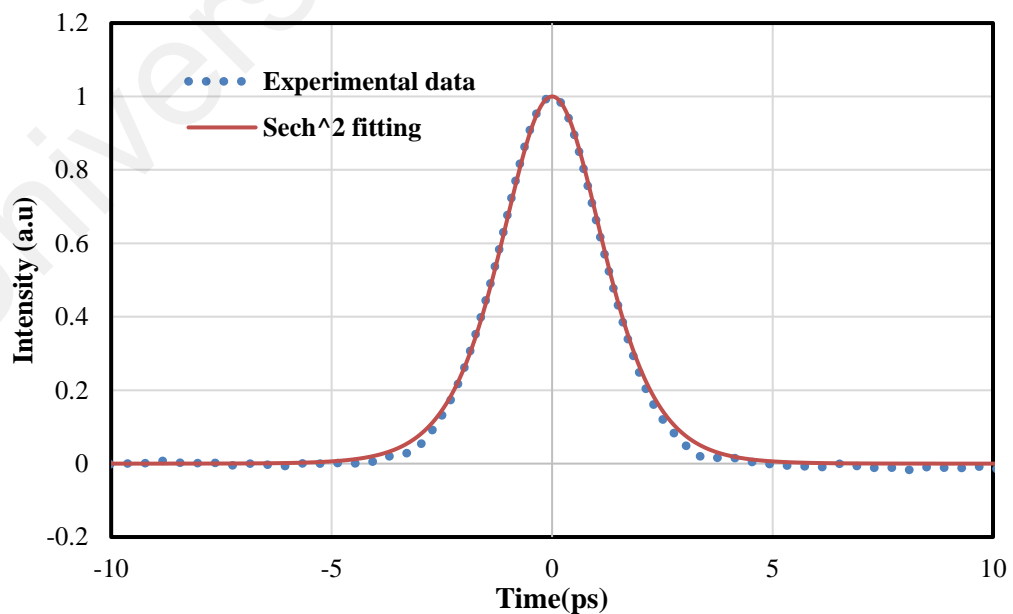


**Figure 4.4 Autocorrelation trace of the mode-locked EDFL at a pump power of 159 mW.**

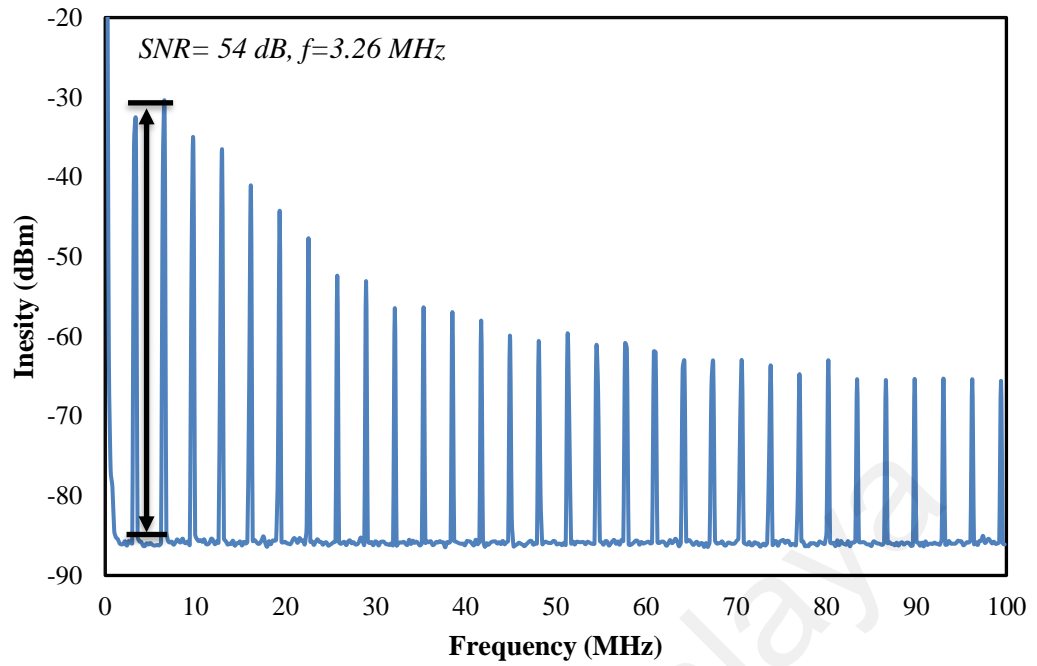


Figure 4.5 RF spectrum of the mode locked at 159 mW.

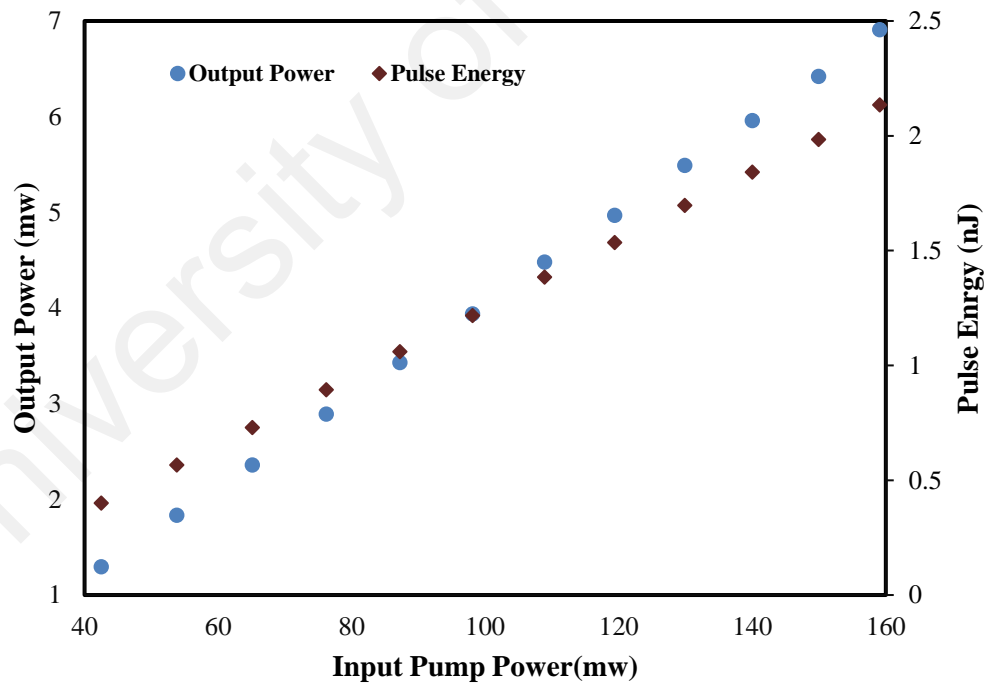


Figure 4.6 Output power and pulse energy as a function of 980nm pump power

#### 4.4 Summary

To sum up this chapter, the same fabricated ZnO thin film is integrated inside a different EDFL's cavity with a shorter length of 61.5 m. Self-started mode locked pulses are generated at a low pump power of 42 mW. The laser operates in the L-band with a central wavelength of 1599.5nm and it has a fundamental frequency and pulse duration of 3.26 MHz and 1.76 ps, respectively. While the pulse energy and peak power of the laser output have been estimated at 2.13 nJ and 1.14 kW respectively at a maximum pump power of 159 mW where the average output power is 6.91 mW. Therefore, the proposed laser can be seen as a promising light source in the emerging optical communication system.

University of Malaya

## CHAPTER 5: CONCLUSION

Fiber lasers gained a lot of interest last two decades to what they got from very attractive advantages such as reliability, compactness, zero alignments, low cost, high output and peak power and lowest coupling loss into the optical communication system. Consequently, they become essential devices in many fields such as engineering technology, laser welding, cutting, and folding of metals, 3D printing, spectroscopy, medicine and optical communication. One of the most developed fiber lasers is Erbium-doped fiber laser (EDFL), and that backs to the desirable wavelength of operation around  $1.5\mu\text{m}$  where silica optical fibers have the lowest attenuation at this range. Therefore, EDFLs gained a huge interest in fiber sensor and optical communication applications.

EDFLs can operate in CW or pulsed mode. However, pulsed lasers are much preferred over CW lasers to what they provide from high peak powers with high repetition rates and short pulse widths. Those specific properties paved the way for pulsed lasers to be used in many applications ranging from basic research to very advanced and sensitive applications such as laser surgery, cutting, welding, range finding, optical communication, and fiber sensing. Q-switching and mode locking are the two mechanisms that usually used to achieve pulsed mode operation. Yet, mode locked EDFLs have the advantages of higher peak powers, much higher repetition rates and extremely short pulse widths. Mode locking pulses can be released using either passive or active techniques. Active techniques are bulky, complicated, expensive, and it limits the pulse width. While passive techniques using saturable absorbers are simpler, cheaper and can provide shorter pulse width than active techniques. In this work, we have fabricated ZnO using seeding solution. And for the purpose of easily integrate the ZnO in the laser cavity, it was formed into a thin film by mixing the seeding solution with the PVA solution. Then, the fabricated ZnO thin film was characterized using FESEM,

Raman spectrum, Wight light source and balance twin detector technique. It is found that ZnO has a linear absorption around 3.5 dB within the operation wavelength range of the EDF. While the modulation depth and saturation intensity are being estimated to be around 5% and 60 MW/cm<sup>2</sup>, respectively.

A small piece of the fabricated ZnO thin film was used first to demonstrate nanosecond mode locked EDFL through integrating it between two clean ferrule connectors inside the laser cavity of 201.5m long forming the saturable absorber. Then, at a relatively low pump power of 45.5 mW, a stable self-started mode locking pulses of 400 ns pulse width were realized, and the fundamental frequency was 993 kHz. While the central wavelength was measured at 1558.34 nm. Furthermore, the proposed lasers' pulse energy and peak power at the maximum available pump power of 142 mW were estimated to be 11.6 nJ and 27.3 mW, respectively. These results show that ZnO thin film is a promising SA for producing nanosecond mode locked EDFL for the applications that required high pulse energy and average output power.

In another experiment, picoseconds mode locking pulses are also being released using different laser cavity of 61.5 m long. After integrating the ZnO thin film inside the new laser cavity, self- started mode locked pulses have been generated at a relatively low pump power of 42 mW with a fundamental frequency and pulse width of 3.26 MHz and 1.76 ps, respectively. The laser operates in the L-band with a central wavelength of 1599.5 nm. The pulse energy and peak power of the laser output have been estimated at 2.16 nJ and 1.14 kW respectively at a maximum pump power of 159 mW where the average output power is 6.91 mW. Based on these results, we believe that the proposed laser can be seen as a promising light source in the emerging optical communication system.

As a future work, ZnO-SA could be tested to generate mode locked pulses in both yttrium and thulium doped fiber lasers of 1  $\mu$ m and 2  $\mu$ m wavelength ranges, respectively.

## REFERENCES

- Adel, P. (2004). *Pulsed Fiber Lasers*: Cuvillier.
- Ahmad, H., Lee, C., Ismail, M., Ali, Z., Reduan, S., Ruslan, N., & Harun, S. (2016). Tunable Q-switched fiber laser using zinc oxide nanoparticles as a saturable absorber. *Applied optics*, 55(16), 4277-4281.
- Ahmad, H., Lee, C., Ismail, M., Ali, Z., Reduan, S., Ruslan, N., . . . Harun, S. (2016). Zinc oxide (ZnO) nanoparticles as saturable absorber in passively Q-switched fiber laser. *Optics Communications*, 381, 72-76.
- Ahmad, H., Reduan, S. A., Ali, Z. A., Ismail, M., Ruslan, N., Lee, C., . . . Harun, S. (2016). C-Band Q-Switched Fiber Laser Using Titanium Dioxide (TiO<sub>2</sub>) As Saturable Absorber. *IEEE Photonics Journal*, 8(1), 1-7.
- Ahmad, H., Salim, M., Ismail, M., & Harun, S. (2016). Q-switched ytterbium-doped fiber laser with zinc oxide based saturable absorber. *Laser physics*, 26(11), 115107.
- Ahmed, M., Ali, N., Salleh, Z., Rahman, A., Harun, S., Manaf, M., & Arof, H. (2014). All fiber mode-locked Erbium-doped fiber laser using single-walled carbon nanotubes embedded into polyvinyl alcohol film as saturable absorber. *Optics & Laser Technology*, 62, 40-43.
- Ahmed, M., Latiff, A., Arof, H., & Harun, S. (2016). Ultrafast erbium-doped fiber laser mode-locked with a black phosphorus saturable absorber. *Laser Physics Letters*, 13(9), 095104.
- Ahmed, M. H. M. (2015). *Development of Q-Switched and Mode-locked Erbium Doped Fiber Lasers Based on Carbon Nanotubes Saturable Absorbers*. Jabatan Kejuruteraan Elektrik, Fakulti Kejuruteraan, Universiti Malaya.
- Ahmed, Z., Tucker, R., Zhai, L., Lowery, A., & Onodera, N. (1992). *Effect of cavity length on the locking bandwidth of high repetition rate mode-locked semiconductor lasers*. Paper presented at the Semiconductor Laser Conference, 1992. Conference Digest. 13th IEEE International.
- Al-Hayali, S. K. M., Mohammed, D. Z., Khaleel, W. A., & Al-Janabi, A. H. (2017). Aluminum oxide nanoparticles as saturable absorber for C-band passively Q-switched fiber laser. *Applied optics*, 56(16), 4720-4726.
- Altshuler, G. B., Erofeev, A. V., & Yaroslavsky, I. (2004). Fiber laser device for medical/cosmetic procedures: Google Patents.
- Aneesh, P., Vanaja, K., & Jayaraj, M. (2007). *Synthesis of ZnO nanoparticles by hydrothermal method*. Paper presented at the Proc. SPIE.
- Arahira, S., Matsui, Y., & Ogawa, Y. (1996). Mode-locking at very high repetition rates more than terahertz in passively mode-locked distributed-Bragg-reflector laser diodes. *IEEE Journal of quantum electronics*, 32(7), 1211-1224.

- Aziz, N., Latiff, A., Lokman, M., Hanafi, E., & Harun, S. (2017). Zinc Oxide-Based Q-Switched Erbium-Doped Fiber Laser. *Chinese Physics Letters*, 34(4), 044202.
- Bagnall, D., Chen, Y., Zhu, Z., Yao, T., Koyama, S., Shen, M. Y., & Goto, T. (1997). Optically pumped lasing of ZnO at room temperature. *Applied Physics Letters*, 70(17), 2230-2232.
- Boguslawski, J., Sobon, G., Zybala, R., & Sotor, J. (2015). Dissipative soliton generation in Er-doped fiber laser mode-locked by Sb<sub>2</sub>Te<sub>3</sub> topological insulator. *Optics letters*, 40(12), 2786-2789.
- Bose, S., & Barua, A. (1999). The role of ZnO: Al films in the performance of amorphous-silicon based tandem solar cells. *Journal of Physics D: Applied Physics*, 32(3), 213.
- Bret, G., & Gires, F. (1964). Giant-pulse laser and light amplifier using variable transmission coefficient glasses as light switches. *Applied Physics Letters*, 4(10), 175-176.
- Cai, J.-H., Chen, H., Chen, S.-P., & Hou, J. (2017). State distributions in two-dimensional parameter spaces of a nonlinear optical loop mirror-based, mode-locked, all-normal-dispersion fiber laser. *Optics express*, 25(4), 4414-4428.
- Cantello, M., Rivela, C., & Penasa, M. (2001). *Industrial applications of lasers*. Paper presented at the XIII International Symposium on Gas Flow and Chemical Lasers and High-Power Laser Conference.
- Chen, L., Zhang, M., Zhou, C., Cai, Y., Ren, L., & Zhang, Z. (2009). *Ultra-low repetition rate SESAM-mode-locked linear-cavity erbium-doped fiber laser*. Paper presented at the Conference on Lasers and Electro-Optics/Pacific Rim.
- Chong, A., Buckley, J., Renninger, W., & Wise, F. (2006). All-normal-dispersion femtosecond fiber laser. *Optics express*, 14(21), 10095-10100.
- Coleman, V., & Jagadish, C. (2006). Basic properties and applications of ZnO. *Zinc Oxide Bulk, Thin Films and Nanostructures: Processing, Properties, and Applications*, 1-20.
- Das, D., & Mondal, P. (2014). Photoluminescence phenomena prevailing in c-axis oriented intrinsic ZnO thin films prepared by RF magnetron sputtering. *RSC Advances*, 4(67), 35735-35743.
- Dausinger, F., & Lichtner, F. (2004). *Femtosecond technology for technical and medical applications* (Vol. 96): Springer Science & Business Media.
- Desurvire, E., Giles, C. R., Simpson, J. R., & Zyskind, J. L. (1991). Erbium-doped fiber amplifier: Google Patents.
- DiDomenico Jr, M. (1964). Small-signal analysis of internal (coupling-type) modulation of lasers. *Journal of Applied Physics*, 35(10), 2870-2876.



- Ding, J., Liu, J., Wei, X., & Xu, J. (2017). *The SMAT Fiber Laser for Industrial Applications*. Paper presented at the Proc. of SPIE Vol.
- Dong, L., & Samson, B. (2016). *Fiber Lasers: Basics, Technology, and Applications*: Crc Press.
- El\_Mashade, M., & Mohamed, A. (2017). *Characteristics Evaluation of Multi-Stage Optical Amplifier EDFA* (Vol. 19).
- Feng, T., Mao, D., Cui, X., Li, M., Song, K., Jiang, B., . . . Quan, W. (2016). A Filmy Black-Phosphorus Polyimide Saturable Absorber for Q-Switched Operation in an Erbium-Doped Fiber Laser. *Materials*, 9(11), 917.
- Fermann, M. E., Galvanauskas, A., & Sucha, G. (2002). *Ultrafast lasers: Technology and applications* (Vol. 80): CRC Press.
- Gao, C., Wang, Z., Luo, H., & Zhan, L. (2017). High Energy All-Fiber Tm-Doped Femtosecond Soliton Laser Mode-Locked by Nonlinear Polarization Rotation. *Journal of Lightwave technology*, 35(14), 2988-2993.
- Gao, L., Zhu, T., Huang, W., & Luo, Z. (2015). Stable, Ultrafast Pulse Mode-Locked by Topological Insulator  $\text{Bi}_2\text{Se}_3$  Nanosheets Interacting With Photonic Crystal Fiber: From Anomalous Dispersion to Normal Dispersion. *IEEE Photonics Journal*, 7(1), 1-8.
- Guerreiro, P., Ten, S., Borrelli, N., Butty, J., Jabbour, G., & Peyghambarian, N. (1997). PbS quantum-dot doped glasses as saturable absorbers for mode locking of a Cr: forsterite laser. *Applied Physics Letters*, 71(12), 1595-1597.
- Haripadmam, P., John, H., Philip, R., & Gopinath, P. (2014). Switching of absorptive nonlinearity from reverse saturation to saturation in polymer-ZnO nanotop composite films. *Applied Physics Letters*, 105(22), 221102.
- Hasan, T., Sun, Z., Wang, F., Bonaccorso, F., Tan, P. H., Rozhin, A. G., & Ferrari, A. C. (2009). Nanotube-polymer composites for ultrafast photonics. *Advanced Materials*, 21(38-39), 3874-3899.
- Ismail, M. A., Harun, S. W., Zulkepely, N. R., Nor, R. M., Ahmad, F., & Ahmad, H. (2012). Nanosecond soliton pulse generation by mode-locked erbium-doped fiber laser using single-walled carbon-nanotube-based saturable absorber. *Applied optics*, 51(36), 8621-8624.
- Jagadish, C., & Pearton, S. J. (2011). *Zinc oxide bulk, thin films and nanostructures: processing, properties, and applications*: Elsevier.
- Jamdagni, P., Khatri, P., & Rana, J. (2016). Green synthesis of zinc oxide nanoparticles using flower extract of *Nyctanthes arbor-tristis* and their antifungal activity. *Journal of King Saud University-Science*.
- Janotti, A., & Van de Walle, C. G. (2009). Fundamentals of zinc oxide as a semiconductor. *Reports on progress in physics*, 72(12), 126501.

- Johnson, J. C., Knutsen, K. P., Yan, H., Law, M., Zhang, Y., Yang, P., & Saykally, R. J. (2004). Ultrafast carrier dynamics in single ZnO nanowire and nanoribbon lasers. *Nano Letters*, 4(2), 197-204.
- Laming, R., Farries, M., Morkel, P., Reekie, L., Payne, D., Scrivener, P., . . . Righetti, A. (1989). Efficient pump wavelengths of erbium-doped fibre optical amplifier. *Electronics Letters*, 25(1), 12-14.
- Lin, J.-H., Chen, Y.-J., Lin, H.-Y., & Hsieh, W.-F. (2005). Two-photon resonance assisted huge nonlinear refraction and absorption in ZnO thin films. *Journal of Applied Physics*, 97(3), 033526.
- Lin, J.-H., Huang, C.-C., & Lin, K.-H. (2010). Characteristics of Q-switched and mode-locked pulses generation in c-cut Nd: LuVO<sub>4</sub> laser by acousto-optic modulator. *Laser physics*, 20(10), 1881-1885.
- Luo, A. P., Luo, Z. C., Xu, W. C., Dvoyrin, V., Mashinsky, V., & Dianov, E. (2011). Tunable and switchable dual-wavelength passively mode-locked Bi-doped all-fiber ring laser based on nonlinear polarization rotation. *Laser Physics Letters*, 8(8), 601-605.
- Luo, Z., Li, Y., Zhong, M., Huang, Y., Wan, X., Peng, J., & Weng, J. (2015). Nonlinear optical absorption of few-layer molybdenum diselenide (MoSe<sub>2</sub>) for passively mode-locked soliton fiber laser. *Photonics Research*, 3(3), A79-A86.
- Maiman, T. H. (1960). Stimulated optical radiation in ruby. *nature*, 187(4736), 493-494.
- Mao, D., Liu, X., Wang, L., Lu, H., & Feng, H. (2010). Generation and amplification of high-energy nanosecond pulses in a compact all-fiber laser. *Optics express*, 18(22), 23024-23029.
- Mao, D., She, X., Du, B., Yang, D., Zhang, W., Song, K., . . . Zhao, J. (2016). Erbium-doped fiber laser passively mode locked with few-layer WSe<sub>2</sub>/MoSe<sub>2</sub> nanosheets. *Scientific reports*, 6, 23583.
- Mao, D., Wang, Y., Ma, C., Han, L., Jiang, B., Gan, X., . . . Zhao, J. (2015). WS<sub>2</sub> mode-locked ultrafast fiber laser. *Scientific reports*, 5.
- McClung, F., & Hellwarth, R. (1962). Giant optical pulsations from ruby. *Applied optics*, 1(101), 103-105.
- Mears, R., Reekie, L., Poole, S., & Payne, D. (1986). Low-threshold tunable CW and Q-switched fibre laser operating at 1.55  $\mu\text{m}$ . *Electronics Letters*, 22(3), 159-160.
- Mears, R. J., Reekie, L., Jauncey, I., & Payne, D. N. (1987). Low-noise erbium-doped fibre amplifier operating at 1.54  $\mu\text{m}$ . *Electronics Letters*, 23(19), 1026-1028.
- Mizrahi, V., DiGiovanni, D. J., Atkins, R. M., Grubb, S. G., Park, Y.-K., & Delavaux, J.-M. (1993). Stable single-mode erbium fiber-grating laser for digital communication. *Journal of Lightwave technology*, 11(12), 2021-2025.

- Montenegro, D., Hortelano, V., Martínez, O., Martínez-Tomas, M., Sallet, V., Muñoz-Sanjosé, V., & Jiménez, J. (2013). Non-radiative recombination centres in catalyst-free ZnO nanorods grown by atmospheric-metal organic chemical vapour deposition. *Journal of Physics D: Applied Physics*, 46(23), 235302.
- Ngo, N. Q. (2010). *Ultra-fast fiber lasers: principles and applications with MATLAB® models*: CRC Press.
- Osellame, R., Cerullo, G., & Ramponi, R. (2012). *Femtosecond laser micromachining: photonic and microfluidic devices in transparent materials* (Vol. 123): Springer Science & Business Media.
- Paschotta, R., Nilsson, J., Tropper, A. C., & Hanna, D. C. (1997). Ytterbium-doped fiber amplifiers. *IEEE Journal of quantum electronics*, 33(7), 1049-1056.
- Patel, R. S., & Bovatsek, J. (2007). Processing benefits of high repetition rate and high average power 355 nm laser for micromachining of microelectronics packaging materials. *Procs. SPIE*, 6419.
- Popa, D., Sun, Z., Torrisi, F., Hasan, T., Wang, F., & Ferrari, A. (2010). Sub 200 fs pulse generation from a graphene mode-locked fiber laser. *Applied Physics Letters*, 97(20), 203106.
- Qingsong, J., Tianshu, W., Wanzhuo, M., Zhen, W., Qingchao, S., Baoxue, B., & Huilin, J. (2017). Mode-Locking Thulium-Doped Fiber Laser With 1.78-GHz Repetition Rate Based on Combination of Nonlinear Polarization Rotation and Semiconductor Saturable Absorber Mirror. *IEEE Photonics Journal*, 9(3), 1-8.
- Quimby, R. S. (2006). *Photonics and lasers: an introduction*: John Wiley & Sons.
- Renninger, W. H., Chong, A., & Wise, F. W. (2008). Giant-chirp oscillators for short-pulse fiber amplifiers. *Optics letters*, 33(24), 3025-3027.
- Sangeetha, G., Rajeshwari, S., & Venkatesh, R. (2011). Green synthesis of zinc oxide nanoparticles by aloe barbadensis miller leaf extract: Structure and optical properties. *Materials Research Bulletin*, 46(12), 2560-2566.
- Sharma, P. K., Dutta, R. K., Choudhary, R., & Pandey, A. C. (2013). Doping, strain, defects and magneto-optical properties of Zn  $1-x$  Mn  $x$  O nanocrystals. *CrystEngComm*, 15(22), 4438-4447.
- Silfvast, W. T. (2004). *Laser fundamentals*: Cambridge university press.
- Soffer, B. (1964). Giant pulse laser operation by a passive, reversibly bleachable absorber. *Journal of Applied Physics*, 35(8), 2551-2551.
- Song, H., Wang, Q., Zhang, Y., & Li, L. (2017). Mode-locked ytterbium-doped all-fiber lasers based on few-layer black phosphorus saturable absorbers. *Optics Communications*, 394, 157-160.

- Sun, X., He, J., Jia, Z., Ning, J., Zhao, R., Su, X., . . . Zhao, S. (2017). Dual-wavelength synchronously mode-locked Nd: LaGGG laser operating at 1.3  $\mu\text{m}$  with a SESAM. *RSC Advances*, 7(51), 32044-32048.
- Sun, Z., Hasan, T., Torrisi, F., Popa, D., Privitera, G., Wang, F., . . . Ferrari, A. C. (2009). Graphene mode-locked ultrafast laser. *arXiv preprint arXiv:0909.0457*.
- Sun, Z., Hasan, T., Torrisi, F., Popa, D., Privitera, G., Wang, F., . . . Ferrari, A. C. (2010). Graphene mode-locked ultrafast laser. *ACS nano*, 4(2), 803-810.
- Svelto, O., & Hanna, D. C. (1998). *Principles of lasers* (Vol. 4): Springer.
- Swann, W. C., Baumann, E., Giorgetta, F. R., & Newbury, N. R. (2011). Microwave generation with low residual phase noise from a femtosecond fiber laser with an intracavity electro-optic modulator. *Optics express*, 19(24), 24387-24395.
- Ter-Mikirtychev, V. (2013). *Fundamentals of fiber lasers and fiber amplifiers* (Vol. 181): Springer.
- Van Dijken, A., Meulenkaamp, E., Vanmaekelbergh, D., & Meijerink, A. (2000). Identification of the transition responsible for the visible emission in ZnO using quantum size effects. *Journal of Luminescence*, 90(3), 123-128.
- Wang, Z. L. (2004). Functional oxide nanobelts: materials, properties and potential applications in nanosystems and biotechnology. *Annu. Rev. Phys. Chem.*, 55, 159-196.
- Woodward, R., Kelleher, E., Runcorn, T., Loranger, S., Popa, D., Wittwer, V., . . . Taylor, J. (2015). Fiber grating compression of giant-chirped nanosecond pulses from an ultra-long nanotube mode-locked fiber laser. *Optics letters*, 40(3), 387-390.
- Woodward, R. I., & Kelleher, E. J. (2015). 2D saturable absorbers for fibre lasers. *Applied Sciences*, 5(4), 1440-1456.
- Xia, H., Li, H., Wang, Z., Chen, Y., Zhang, X., Tang, X., & Liu, Y. (2014). Nanosecond pulse generation in a graphene mode-locked erbium-doped fiber laser. *Optics Communications*, 330, 147-150.
- Xu, J., Wu, S., Liu, J., Wang, Q., Yang, Q.-H., & Wang, P. (2012). Nanosecond-pulsed erbium-doped fiber lasers with graphene saturable absorber. *Optics Communications*, 285(21), 4466-4469.
- Yin, K., Zhang, B., Li, L., Jiang, T., Zhou, X., & Hou, J. (2015). Soliton mode-locked fiber laser based on topological insulator Bi<sub>2</sub>Te<sub>3</sub> nanosheets at 2  $\mu\text{m}$ . *Photonics Research*, 3(3), 72-76.
- Zhong, Y., Zhang, Z., & Tao, X. (2010). Passively mode-locked fiber laser based on nonlinear optical loop mirror with semiconductor optical amplifier. *Laser physics*, 20(8), 1756-1759.

Zirngibl, M., Stulz, L., Stone, J., Hugi, J., DiGiovanni, D., & Hansen, P. (1991). 1.2 ps pulses from passively mode-locked laser diode pumped Er-doped fibre ring laser. *Electronics Letters*, 27(19), 1734-1735.

University of Malaya

## LIST OF PUBLICATIONS AND PAPERS PRESENTED

1. **Alani, I. A. M.**, Ahmed M. H. M., Latiff, A. A., Lokman, M. Q. Al-Masoodi, A. H. H., and Harun, S. W (2017). A Few Picosecond and High Peak Power of Passively Mode-locked Erbium-doped Fiber Laser based on Zinc Oxide Polyvinyl Alcohol Film Saturable Absorber. *Laser physics*, (Revised).
2. **Alani, I. A. M.**, Ahmed, M. H. M., Latiff, A. A., Al-Masoodi, A. H. H., Lokman, M. Q. and Harun S. W. (2017). Nanosecond mode-locked Erbium Doped Fiber Laser based on Zinc Oxide (ZnO) thin film as a Saturable Absorber. *Indian Journal of Physics*, (Revised).
3. Al-Masoodi, H. H., Ahmad, F., Ahmed, M. H. M., Al-Masoodi, A. H. H., **Alani, I. A. M.**, Arof, H., Harun, S. W. (2017). Q-switched and mode-locked Ytterbium doped fiber lasers With Sb<sub>2</sub>Te<sub>3</sub> topological insulator saturable absorber. *IET Optoelectronics*. (Revised).